

Online Bayesian changepoint detection for network Poisson processes with community structure

Joshua Corneck, Edward A. K. Cohen, James S. Martin, and Francesco Sanna Passino

Department of Mathematics, Imperial College London
180 Queen's Gate, SW7 2AZ, London

This is a pre-print of an article published in Statistics and Computing. The final authenticated version is available online at: <https://doi.org/10.1007/s11222-025-10606-w>.

Abstract

Network point processes often exhibit latent structure that govern the behaviour of the sub-processes. It is not always reasonable to assume that this latent structure is static, and detecting when and how this driving structure changes is often of interest. In this paper, we introduce a novel online methodology for detecting changes within the latent structure of a network point process. We focus on block-homogeneous Poisson processes, where latent node memberships determine the rates of the edge processes. We propose a scalable variational procedure which can be applied on large networks in an online fashion via a Bayesian forgetting factor applied to sequential variational approximations to the posterior distribution. The proposed framework is tested on simulated and real-world data, and it rapidly and accurately detects changes to the latent edge process rates, and to the latent node group memberships, both in an online manner. In particular, in an application on the Santander Cycles bike-sharing network in central London, we detect changes within the network related to holiday periods and lockdown restrictions between 2019 and 2020.

Keywords — network point process, online variational inference, stochastic blockmodel, streaming data.

1 Introduction

Network data describe complex relationships between a large number of entities, called *nodes*, linked via *edges*. In particular, much of such data is continuous-time valued and dynamic in nature, with nodes often exhibiting a latent *community structure* that drives interactions (Amini et al., 2013). By allowing temporal point processes to exist on the edges of the network, and not solely focusing on the adjacency matrix, such interaction data can be more accurately understood. Common examples of these network structures include email exchanges within a company (Klimt and Yang, 2004) or posts on a social media platform (Paranjape et al., 2017), where employer hierarchy or political leanings, respectively, could drive connections between individuals. Furthermore, it is not always reasonable to assume that such structure is static. In the case of email exchanges, a change in an employee's role within their organisation would alter the latent community structure of the network. Similarly, in social networks, a sporting or political event would likely affect the frequency of interactions only between users with particular characteristics and topics of interest. Detecting such changepoints is crucial in many real-world applications, such as in the context of computer networks, where modifications of network structure can signify malicious behaviour (see, for example, Hallgren et al., 2023). The detection of such changes in an online manner will be the focus of this paper.

Much of the original work on network models focused on simple, binary connections between nodes. One of the most common of these modelling approaches is the Stochastic Block Model (SBM; Holland et al., 1983), which models connections between nodes via a latent community structure on a network. This model has undergone significant development, with theoretical results extending to include node degree heterogeneity

(Karrer and Newman, 2011; Amini et al., 2013; Gao et al., 2018), valued edges (Mariadassou et al., 2010), dynamic community structure in discrete time (Matias and Miele, 2017; Yang et al., 2011; Xu and Hero, 2014), and missing data (Mariadassou and Tabouy, 2020); refer to Lee and Wilkinson (2019) for a comprehensive review. In spite of their simplicity, SBMs can be used to consistently estimate and approximate much more complex network objects, such as exchangeable random graphs and their associated graphons, and thus provide a good approximation for any exchangeable random graph model (Airoldi et al., 2013). However, most of these advancements are based on aggregated, discrete time data.

There are several statistical methods for analysing dynamic networks, normally defined as graphs with time-evolving edge-connections. Interested readers are referred to Holme (2015) for a review. However, most of this methodology does not capture instantaneous interactions, but relies instead on aggregations (see, for example, Shlomovich et al., 2022). To combat this, Matias et al. (2018) developed a model for recurrent interaction events, which they call the semiparametric stochastic block model. In this framework, interactions are modelled by a conditional inhomogeneous Poisson process, with intensities depending solely on the latent group memberships of the interacting individuals. Perry and Wolfe (2013) uses a Cox multiplicative intensity model with covariates to model the point processes observed on each edge. Sanna Passino and Heard (2023) models the edge-specific processes via mutually exciting processes with intensities depending only on node-specific parameters. These methodologies handle complex temporal data, but they are offline methods, and work only in the case of a static latent network structure. Attempts have been made at capturing networks with a dynamic latent structure, but attention has focused on discrete time data, such as binary or weighted edges. Matias and Miele (2017) proposed a method for frequentist inference for a model which extends the SBM to allow for dynamic group memberships. In that work, the dynamics of the groups are modelled by a discrete time Markov chain. Heard et al. (2010) developed a two-stage offline method for anomaly detection in dynamic graphs. However, to the best of our knowledge, there currently exists no methodology for online detection of changepoints in the context of continuous-time network data.

The recent work of Fang et al. (2024) represents the first attempt at online estimation and community detection of a network point process. The authors build upon the foundation laid by Matias et al. (2018) and extend it to an online setting, but maintain the assumption of a static latent structure. While Fang et al. (2024) do offer suggestions as to how their framework could be extended to incorporate latent dynamics, the methodology developed therein requires knowing both the adjacency matrix and the number of latent groups a priori.

In this work, we propose a novel online Bayesian changepoint detection algorithm for network point processes with a latent community structure among the nodes. Our methodology is based on utilising *forgetting factors* within a Bayesian context to sequentially update the variational approximation to the posterior distribution of the model parameters when new data are observed within a stream. We focus on what we will refer to as a dynamic Bayesian block-homogeneous network Poisson process, where dynamic refers to the fact that the latent structure of the network is time-varying. As an added benefit, our method is able to accurately infer the community structure and obtain a piecewise recovery of the conditional intensity function when we consider inhomogeneous Poisson processes on the edges. Extensions to our method are proposed to infer either the adjacency matrix of the network or the number of latent groups, each in conjunction with the edge rates. We also extend to handle cases where new groups are created or existing ones are merged.

The remainder of this article is structured as follows: Section 2 describes the dynamic Bayesian block-homogeneous Poisson process model used in this work, and the possible local and global changes to the network structure occurring on such a network model. Section 3 discusses the proposed online variational Bayesian inference approach via Bayesian forgetting factor, which is used to sequentially approximate the posterior distribution on the stream. The performance of the proposed inferential procedure is then tested in Section 4 on simulated data, and on real-world data from the Santander Cycles bike-sharing network in Section 5, followed by a discussion.

2 Bayesian dynamic block homogeneous Poisson process

2.1 The model

We consider a stochastic process on a network, which produces dyadic interaction data between a set of N nodes observed over time. Let $\mathcal{G} = (\mathcal{V}, \mathcal{E})$ be a graph, where the set $\mathcal{V} := \{1, \dots, N\}$ corresponds to nodes, whereas the edge set $\mathcal{E} \subseteq \mathcal{V} \times \mathcal{V}$ contains pairs representing interactions between nodes in \mathcal{V} . In particular, we write $(i, j) \in \mathcal{E}$ if there is a connection from node $i \in \mathcal{V}$ to node $j \in \mathcal{V}$. Furthermore, we denote the set of all possible edges between nodes as $\mathcal{R} = \mathcal{V} \times \mathcal{V}$. The graph \mathcal{G} could be equivalently represented via its adjacency matrix $\mathbf{A} = \{a_{ij}\} \in \{0, 1\}^{N \times N}$ such that $a_{ij} = \mathbb{I}_{\mathcal{E}}\{(i, j)\}$, where $\mathbb{I}\{\cdot\}$ denotes the indicator function.

We assume that each node $i \in \mathcal{V}$ belongs to a group $z_i \in \mathcal{K}$, where $\mathcal{K} := \{1, \dots, K\}$ and we let $\mathbf{z} = (z_1, \dots, z_N) \in \mathcal{K}^N$ be a priori independent and identically distributed with $z_i \sim \text{Categorical}(\pi)$ where $\pi = (\pi_1, \dots, \pi_K)$, such that $\pi_k \geq 0$ for all $k \in \mathcal{K}$, and $\sum_{k=1}^K \pi_k = 1$. We also associate to z_i a binary vector $\tilde{z}_i = (\tilde{z}_{i1}, \dots, \tilde{z}_{iK}) \in \{0, 1\}^K$, with $\tilde{z}_{ik} = \mathbb{I}_{\{k\}}(z_i)$, and we write $\tilde{\mathbf{Z}} = \{\tilde{z}_{ik}\}_{i \in \mathcal{V}, k \in \mathcal{K}} \in \{0, 1\}^{N \times K}$ to denote the matrix of group memberships. Denote by $\Pi = (\Pi_1, \dots, \Pi_K)$ a vector of the proportion of N attributed to each group. Under a Bayesian framework, we place a Dirichlet prior distribution on π with parameter $\gamma^0 \in \mathbb{R}_+^K$.

We observe a marked point process on the network, consisting of a stream of triplets $(i_\ell, j_\ell, t_\ell) \in \mathcal{E} \times \mathbb{R}_+$, $\ell = 1, 2, \dots$, denoting directed interactions from node i_ℓ to node j_ℓ at time t_ℓ , where $t_\ell \leq t_{\ell'}$ for $\ell < \ell'$. The associated edge-specific counting process is denoted by $x_{ij}(\cdot)$, where, for all $(i, j) \in \mathcal{E}$,

$$x_{ij}((0, t]) \equiv x_{ij}(t) := \sum_{\ell} \mathbb{I}_{\{(i, j)\}}\{(i_\ell, j_\ell)\} \mathbb{I}_{(0, t]}(t_\ell).$$

If $(i, j) \notin \mathcal{E}$, $x_{ij}(t) = 0$ for the entire observation period. In this work, we model the counting process $x_{ij}(\cdot)$ as a Poisson process with rate $\lambda_{z_i z_j} \in \mathbb{R}_+$, conditional on $(i, j) \in \mathcal{E}$ and on the node group memberships z_i and z_j . Also, we place independent conjugate gamma prior distributions on the event rates $\lambda = \{\lambda_{km}\} \in \mathbb{R}_+^{K \times K}$. In summary, the full model can be expressed as follows:

$$x_{ij}(t) \mid z_i, z_j, \lambda_{z_i z_j} \sim \text{Poisson}(\lambda_{z_i z_j} t), \quad \text{for all } (i, j) \in \mathcal{E}, \quad (2.1)$$

$$\lambda_{km} \sim \text{Gamma}(\alpha_{km}^0, \beta_{km}^0), \quad \text{for all } k, m \in \mathcal{K}, \quad (2.2)$$

$$z_i \mid \pi \sim \text{Categorical}(\pi), \quad \text{for all } i \in \mathcal{V},$$

$$\pi \sim \text{Dirichlet}(\gamma^0), \quad (2.3)$$

where $\gamma^0 = (\gamma_1^0, \dots, \gamma_K^0) \in \mathbb{R}_+^K$, $\alpha^0 = \{\alpha_{km}^0\}_{k, m \in \mathcal{K}} \in \mathbb{R}_+^{K \times K}$ and $\beta^0 = \{\beta_{km}^0\}_{k, m \in \mathcal{K}} \in \mathbb{R}_+^{K \times K}$. Note that in (2.1), we use that for a homogeneous Poisson process with rate λ^* , the number of counts for that process on an interval of length t is Poisson distributed with rate $\lambda^* t$. The model for $x_{ij}(t)$ in (2.1) is known as the *block homogeneous Poisson process* (BHPP; Fang et al., 2024). The full Bayesian model in (2.1)-(2.3) is represented in graphical model form in Figure 1.

Under the BHPP, the expected waiting time between events across the entire network is $\mathcal{O}(N^{-1})$, as described in the following proposition.

Proposition 1. *Let $\mathcal{G} = (\mathcal{V}, \mathcal{E})$ be a directed graph with no isolated nodes. If on each edge lives a homogeneous Poisson process with rate $\lambda_{z_i z_j} \in \mathbb{R}_+$, only dependent upon node memberships $z_i, z_j \in \mathcal{K}$, then the expected waiting time between arrivals for the full network counting process $x(t) = \sum_{(i, j) \in \mathcal{E}} x_{ij}(t)$ is $\mathcal{O}(N^{-1})$.*

Proof. Let $\mathcal{G} = (\mathcal{V}, \mathcal{E})$ with $|\mathcal{V}| = N$. Suppose that \mathcal{G} has M connected components. As we have no isolated nodes, the number of edges is minimised with $M = N/2$ and $|\mathcal{E}| = N/2$ if N is even, or $M = (N - 1)/2$ and $|\mathcal{E}| = (N + 1)/2$, if N is odd. Without loss of generality, assume $\lambda_{11} = \min_{k, m \in \mathcal{K}} \{\lambda_{km}\}$ and call the rate of the full network Poisson process λ . By superposition, it follows $\lambda \geq N\lambda_{11}/2$ or $\lambda \geq (N + 1)\lambda_{11}/2$, for n even and odd, respectively, and so the expected waiting time w , is bounded as $w \leq 2/\lambda_{11}N$. \square

The aim of the present paper is to provide an online algorithm for detecting changepoints; such an algorithm must be able to perform inference at each time step before the arrival of any new data. A consequence of

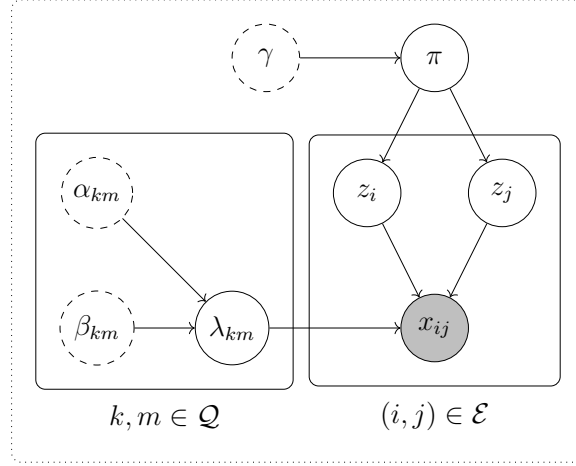


Figure 1: A directed acyclic graphical model representation of the model in Equations (2.1)-(2.3).

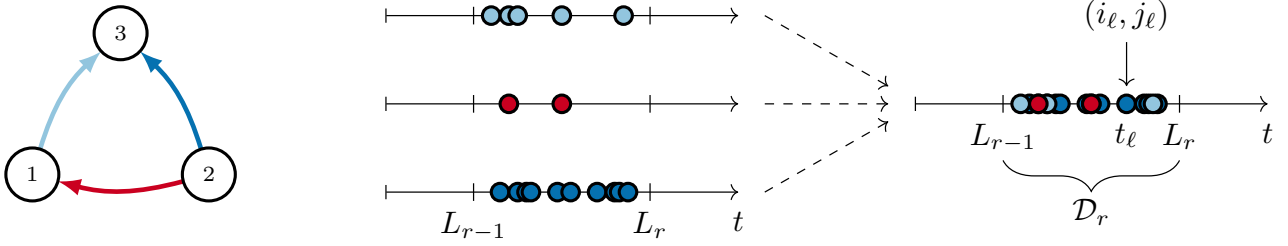


Figure 2: Illustration of the setup in Section 2.1 for a network with $N = 3$ and $\mathcal{E} = \{(1, 3), (2, 1), (2, 3)\}$. Circles represent event times, coloured according to their edge. Arrival times to each edge are collated into \mathcal{D}_r .

Proposition 1 is that for networks of increasing size, this becomes infeasible for large N when observing all events as they arrive, as an online algorithm would need to be at least as fast. This motivates a further assumption that data arrives as a stream of batched counts rather than a stream of continuous-valued event times. Let the batches be observed at times L_r , $r = 1, 2, \dots$, where $L_r < L_{r'}$ for $r < r'$. For $r = 1, 2, \dots$, each data batch takes the form

$$\mathcal{D}_r := \{(i_\ell, j_\ell, t_\ell) : L_{r-1} < t_\ell \leq L_r\}; \quad L_0 \equiv 0.$$

We consider the case of a constant time Δ between batches, so that $L_r - L_{r-1} = \Delta$ for all r . Also, we denote the complete set of data available at time L_r as $\mathcal{D}_{1:r} := \{\mathcal{D}_1, \dots, \mathcal{D}_r\}$. This setup is illustrated in Figure 2.

Initially, we assume that both the adjacency matrix \mathbf{A} and the number of latent groups K are known *a priori*, similar to the setup in Fang et al. (2024). However, we note that assuming this knowledge is limiting in practical applications, since these quantities are usually unknown. Therefore, Sections 3.5 and 3.6 discuss extensions of the BHPP model and corresponding inference procedures with an unknown adjacency matrix and an unknown number of groups.

2.2 Changes to the network

In real-world applications, it is unrealistic to assume that the latent group memberships $\mathbf{z} = (z_1, \dots, z_N)$ and rate matrix $\lambda = \{\lambda_{km}\}_{k,m \in \mathcal{K}}$ are constant across the entire observation period. Our objective is therefore to develop a framework which could be used to detect *global* and *local* changes to the model parameters.

For *local* changes, we consider modifications to the latent group structure, allowing for any $n \leq N$ nodes to change their group membership at any time t' . In contrast to the approach of Matias and Miele (2017), in which the membership of node i over the observation window behaves according to a discrete-time, irreducible and aperiodic Markov chain, we place no model on how or when nodes change and allow for any (finite) number of changes in a given interval. Furthermore, we allow for changes in continuous time, again in contrast to the

discrete-time formulation of [Matias and Miele \(2017\)](#). Our main objective is only to detect if and when nodes have changed memberships, and not to estimate the underlying group membership switching process.

For *global* changes, we consider jumps in the intensity between any groups $k, m \in \mathcal{K}$ at some time $t' \in \mathbb{R}_+$ of the form $\lambda_{km} \mapsto \lambda'_{km}$ ($\lambda_{km} \neq \lambda'_{km}$). Again, we are interested in assessing if the block-specific intensity λ_{km} has changed, and we do not estimate or posit assumptions on the mechanism that leads to such changes.

3 An online variational Bayesian estimation procedure

We present an online inference procedure for tracking the time-evolving latent structure and parameters of the BHPP model described in Section 2.1. We focus first on the set-up where the full edge set \mathcal{E} and the number of latent groups K is known, as in [Fang et al. \(2024\)](#). Next, we consider when \mathcal{E} is unknown, and then we move to the case of an unknown number of groups, using a Bayesian nonparametric approach.

3.1 Variational Bayesian approximation

Variational Bayesian (VB) inference has the objective to approximate a posterior distribution when it is not analytically tractable ([Wang and Blei, 2019](#)), offering a faster estimation approach when compared to Markov Chain Monte Carlo methods ([Blei et al., 2017](#)). This makes it more suited to the requirements of an online learning framework. We adopt the terminology of [Blei et al. \(2017\)](#) in distinguishing between local latent variables z_1, \dots, z_N , that scale with the number of nodes, and global latent variables $\theta = (\pi, \lambda)$, whose dimension, written $S \in \mathbb{N}$, does not change with N .

In a variational approach, one posits a family of distributions \mathcal{F}^{N+S} on the parameter space (θ, z) , and seeks to select the component $q^*(\theta, z) \in \mathcal{F}^{N+S}$ closest to the true posterior $p(\theta, z | x)$ in the sense of the Kullback-Leibler (KL) divergence, where x denotes the observed data. A mathematically convenient choice for \mathcal{F}^{N+S} is the mean-field variational family, the set of factorisable distributions of the form

$$\mathcal{F}^{N+S} = \left\{ q : q(\theta, z) = \prod_{i=1}^N q_{z_i}(z_i) \prod_{s=1}^S q_{\theta_s}(\theta_s) \right\}.$$

The approximating distribution $q^*(\theta, z) \in \mathcal{F}^{N+S}$ is then given as

$$q^*(\theta, z) = \underset{q \in \mathcal{F}^{N+S}}{\operatorname{argmin}} \operatorname{KL} [q(\theta, z) \parallel p(\theta, z | x)]. \quad (3.1)$$

Despite every $q(\theta, z) \in \mathcal{F}^{N+S}$ taking a simple product structure, the solution $q^*(\theta, z)$ to (3.1) is usually not available analytically. A popular method for approximating the global minimum $q^*(\theta, z)$ of the KL-divergence is the Coordinate Ascent Variational Inference (CAVI) algorithm ([Bishop, 2006](#); [Blei et al., 2017](#)), which iteratively updates each component of $q(\theta, z)$ while keeping the others fixed. Letting ϕ denote the $(N + S)$ -dimensional vector of latent variables $\phi = (z, \theta)$, CAVI proceeds as:

$$\hat{q}_{\phi_j}^{(t+1)}(\phi_j) = \underset{q_{\phi_j}}{\operatorname{argmin}} \operatorname{KL} \left[q_{\phi_j}(\phi_j) \prod_{i < j} \hat{q}_{\phi_i}^{(t+1)}(\phi_i) \prod_{i > j} \hat{q}_{\phi_i}^{(t)}(\phi_i) \parallel p(\phi | x) \right], \quad (3.2)$$

for $j \in \{1, \dots, N + S\}$, $t = 0, 1, 2, \dots$ until some convergence criterion is met. Under the mean-field variational approximation, (3.2) has the following solution ([Bishop, 2006](#)):

$$\hat{q}_{\phi_j} \propto \exp\{\mathbb{E}_{-\phi_j} [\log p(x, \phi)]\}, \quad (3.3)$$

where the notation $\mathbb{E}_{-\phi_j}$ used to denote the expectation with respect to all components of ϕ except ϕ_j ([Blei et al., 2017](#)). As per convention with variational inference algorithms, we will drop the subscript on $q_{\phi_j}(\phi_j)$ for notational convenience, and take the argument of the variational component to index it (see, for example, [Blei et al., 2017](#)).

It should be noted that CAVI is only guaranteed to achieve a local minimum, and hence is sensitive to initialisation (Zhang and Zhou, 2020; Blei et al., 2017). Furthermore, with $\phi = (z, \theta)$, updates in (3.3) have an explicit ordering. The ordering of the updates can also have implications on the convergence properties of the algorithm (Ray and Szabó, 2022), similarly to Gibbs sampling (see, for example, van Dyk and Park, 2008).

3.2 Online VB for the dynamic BHPP

Upon receiving the latest batch \mathcal{D}_r at time L_r , the aim of an online algorithm is to update the estimates of the BHPP parameters based on the entire history $\mathcal{D}_{1:r}$ of the process. To ensure finite and constant complexity and memory, a truly online algorithm should be *single pass* (see, for example Bifet et al., 2018): each data batch should be inspected only once, and summaries of previous data batches $\mathcal{D}_{1:(r-1)}$ are used in conjunction with \mathcal{D}_r to update parameter estimates.

The prior-posterior distribution updates within a Bayesian framework offers a natural way to propagate information forward in time. The posterior distribution at time L_{r-1} contains the information that was learned from $\mathcal{D}_{1:(r-1)}$. A naive approach therefore is to pass this through as the new prior distribution for the update at time L_r . However, this will perform poorly in the case of changing latent structure. As the number of batches increases, the new prior distributions become more concentrated around the current best estimates. This results in an updated posterior distribution that is largely dominated by its prior distribution (corresponding to the posterior distribution up to the previous batch) and which is increasingly insensitive to new data and changes in the data generating process.

We therefore propose to flatten the posterior obtained at L_{r-1} , via temperature parameters, at the point of passing it through as the prior distribution for the update at L_r . This flattening step is in effect down-weighting previous observations and can therefore be considered as a Bayesian analogue of the *forgetting factor* procedure that has been widely used in frequentist online literature (see, for example, Haykin, 2002; Bodenham and Adams, 2017). In this way, the parameter estimates are quicker to respond to changes in the latent rate structure.

Due to the independence of counts from a Poisson process within non-overlapping time windows, the posterior density at time step r under the BHPP model factorises as

$$\begin{aligned} p(z, \theta \mid \mathcal{D}_{1:r}) &\propto p(z \mid \pi) p(\pi) p(\lambda) \prod_{\ell=1}^r p(\mathcal{D}_\ell \mid z, \lambda) \\ &\propto p(\mathcal{D}_r \mid z, \lambda) \times p(z, \theta \mid \mathcal{D}_{1:(r-1)}), \end{aligned} \quad (3.4)$$

where the prior distributions are chosen to be conjugate, as per (2.2) and (2.3). From (3.4), the posterior distribution at time step $r - 1$ can be interpreted as the prior for the posterior distribution at time step r .

The posterior density in (3.4) is not available in closed form and, due to the marginal density $p(\mathcal{D}_{1:r})$ being unavailable, can only be evaluated up to a normalising constant. We thus consider the VB approach with the mean-field variational family, deploying the CAVI algorithm to compute approximate posterior distributions. Denoting the approximate posterior at time step $r - 1$ by $\hat{q}^{(r-1)}(\theta, z)$, we pass through as the prior for time step r the *tempered* density

$$\hat{q}_{\delta}^{(r-1)}(\theta, z) = \hat{q}_{\delta_{\pi}}^{(r-1)}(\pi) \times \prod_{k,m \in \mathcal{K}} \hat{q}_{\delta_{\lambda}}^{(r-1)}(\lambda_{km}) \prod_{i \in \mathcal{V}} \hat{q}_{\delta_z}^{(r-1)}(z_i) \quad (3.5)$$

$$\propto \hat{q}^{(r-1)}(\pi)^{\delta_{\pi}} \prod_{k,m \in \mathcal{K}} \hat{q}^{(r-1)}(\lambda_{km})^{\delta_{\lambda}} \prod_{i \in \mathcal{V}} \hat{q}^{(r-1)}(z_i)^{\delta_z}, \quad (3.6)$$

controlled by the *Bayesian forgetting factor* (BFF) $\delta = (\delta_{\lambda}, \delta_z, \delta_{\pi}) \in (0, 1]^3$. Here, C_{r-1} is a normalising constant to ensure a valid density. This procedure is visualised in Figure 3.

The effect of the BFF in down-weighting previous data and placing greater emphasis on the latest batch \mathcal{D}_r is illustrated in Figure 4. A fully-connected network is simulated on the time interval $[0, 5]$ with $N = 500$ nodes and $K = 2$ groups. An instantaneous rate change in λ_{11} is made at $t = 1$. The left panel of Figure 4 shows the results for naive approach (without a forgetting factor), whereas the right panel includes a BFF and demonstrates a much faster response to the change and quicker convergence of the posterior mean to the true value.

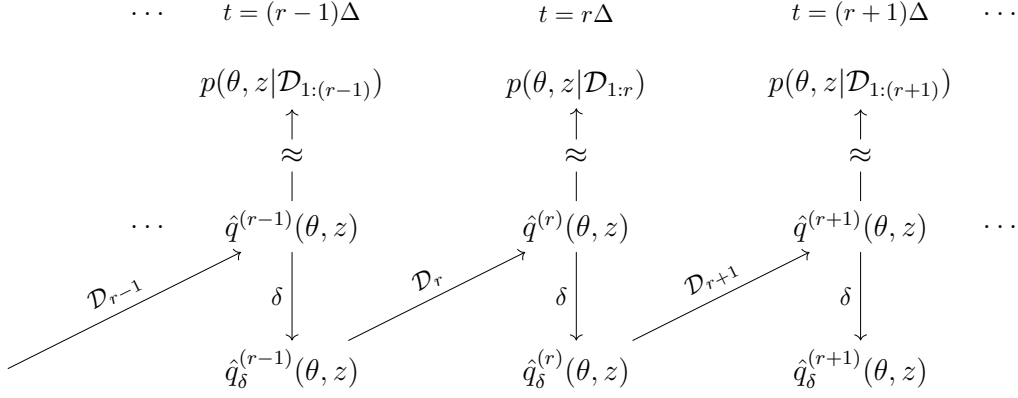


Figure 3: A representation of the transformation of the CAVI approximation from the r -th time step via temperature parameters δ and its use as a prior for the $(r + 1)$ -th time step. The overlaying of \mathcal{D}_r on the diagonal arrows indicates that the transformed CAVI posterior is combined with incoming data to yield the next approximate posterior.

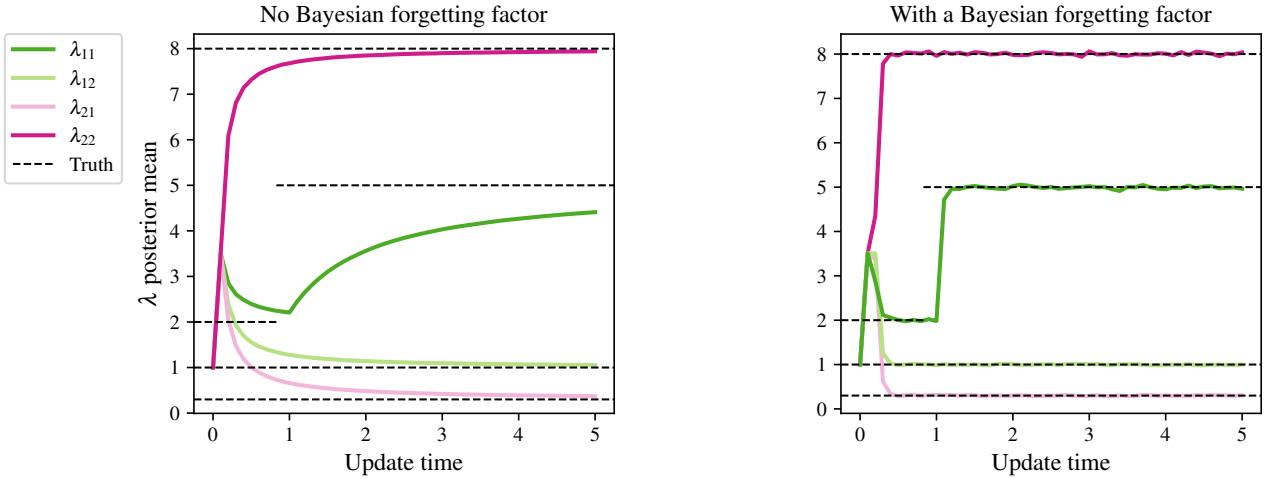


Figure 4: Estimated posterior mean of $\lambda \in \mathbb{R}_+^{K \times K}$ for a fully connected graph with $N = 500$ nodes simulated on $[0, 5]$, with $K = 2$ groups, $\Pi = (0.6, 0.4)$, $\lambda_{22} = 8$, $\lambda_{12} = 1$, $\lambda_{21} = 0.3$, and $\lambda_{11} = 2$. At $t = 1$, λ_{11} changes to 5. The four coloured lines are the posterior means of the components λ , plotted against time step. The black dashed horizontal lines are the true values of λ at each time point. $\delta = 0.1$ in the right-hand panel.

A BFF of 0.1 was found to work well in our simulations, except in the case of very low rates. In this case, where we might see no counts in an interval, one would select δ_λ closer to 1 to allow the prior to inform the estimates. However, our methodology does not require that Δ be fixed, and so in the case of low counts, one could instead allow for a longer waiting period before updating.

3.3 Online CAVI updates

We assume that each component of (3.5) takes the same form of its corresponding complete conditional distribution under the standard BHPP model in (2.1)–(2.3), raised to a power and normalised:

$$\begin{aligned} \hat{q}_{\delta_\lambda}^{(r-1)}(\lambda_{km}) &= \frac{1}{C_{\lambda_{km}, r-1}} \text{Gamma} \left(\alpha_{km}^{(r-1)}, \beta_{km}^{(r-1)} \right)^{\delta_\lambda}, & \text{for all } k, m \in \mathcal{K}, \\ \hat{q}_{\delta_z}^{(r-1)}(z_i) &= \frac{1}{C_{z_i, r-1}} \text{Categorical} \left(\tau_i^{(r-1)} \right)^{\delta_z}, & \text{for all } i \in \mathcal{V}, \end{aligned}$$

$$\hat{q}_{\delta_\pi}^{(r-1)}(\pi) = \frac{1}{C_{\pi,r-1}} \text{Dirichlet} \left(\gamma^{(r-1)} \right)^{\delta_\pi}.$$

The above notation indicates that we take the probability density or mass function of the relevant distribution, raise it to a power and then normalise. $C_{\lambda_{km},r-1}$, $C_{z_i,r-1}$ and $C_{\pi,r-1}$ are normalising constants, ensuring that the densities are valid, and $\delta = (\delta_\lambda, \delta_z, \delta_\pi) \in (0, 1]^3$ are temperature parameters specific to each class of latent variables. Suppose that data is observed on the interval $I_r := (L_{r-1}, L_r]$, for $r \in \mathbb{N}$, and denote the count on edge (i, j) during this interval by $x_{ij}(I_r)$. Under the prior structure in (3.5), it is shown in Appendix A that the CAVI sequential updates are:

1. $\hat{q}^{(r)}(\lambda_{km}) = \text{Gamma} \left(\alpha_{km}^{(r)}, \beta_{km}^{(r)} \right)$ for all $k, m \in \mathcal{K}$ where $\alpha_{km}^{(r)}, \beta_{km}^{(r)}$ are defined as:

$$\begin{aligned} \alpha_{km}^{(r)} &= \delta_\lambda \left(\alpha_{km}^{(r-1)} - 1 \right) + \sum_{(i,j) \in \mathcal{E}} \tau_{ik}^{(r-1)} \tau_{jm}^{(r-1)} x_{ij}(I_r) + 1, \\ \beta_{km}^{(r)} &= \delta_\lambda \beta_{km}^{(r-1)} + \Delta \sum_{(i,j) \in \mathcal{E}} \tau_{ik}^{(r-1)} \tau_{jm}^{(r-1)}. \end{aligned} \quad (3.7)$$

2. $\hat{q}^{(r)}(z_i) = \text{Categorical} \left(\tau_i^{(r)} \right)$ for all $i \in \mathcal{V}$ where $\tau_i^{(r)} = (\tau_{i1}^{(r)}, \dots, \tau_{iK}^{(r)})$, with $\sum_{k \in \mathcal{K}} \tau_{ik}^{(r)} = 1$, satisfies the relation:

$$\begin{aligned} \tau_{ik}^{(r)} &\propto \exp \left\{ \delta_z \left[\psi \left(\gamma_k^{(r-1)} \right) - \psi \left(\sum_{m \in \mathcal{K}} \gamma_m^{(r-1)} \right) \right] + x_{ii}(I_r) \left[\psi \left(\alpha_{kk}^{(r)} \right) - \log \left(\beta_{kk}^{(r)} \right) \right] - \Delta \frac{\alpha_{kk}^{(r)}}{\beta_{kk}^{(r)}} \right. \\ &\quad + \sum_{m \in \mathcal{K}} \left[\sum_{j: (i,j) \in \mathcal{E}} \tau_{jm}^{(r)} \left(x_{ij}(I_r) \left\{ \psi \left(\alpha_{km}^{(r)} \right) - \log \left(\beta_{km}^{(r)} \right) \right\} - \Delta \frac{\alpha_{km}^{(r)}}{\beta_{km}^{(r)}} \right) \right. \\ &\quad \times \left(1 - \mathbb{I}_{\{k\}}(m) \mathbb{I}_{\{i\}}(j) \right) + \sum_{j': (j',i) \in \mathcal{E}} \tau_{j'm}^{(r)} \left(x_{j'i}(I_r) \left\{ \psi \left(\alpha_{mk}^{(r)} \right) - \log \left(\beta_{mk}^{(r)} \right) \right\} - \Delta \frac{\alpha_{mk}^{(r)}}{\beta_{mk}^{(r)}} \right) \\ &\quad \left. \left. \times \left(1 - \mathbb{I}_{\{k\}}(m) \mathbb{I}_{\{i\}}(j') \right) \right] \right\}. \end{aligned} \quad (3.8)$$

3. $\hat{q}^{(r)}(\pi) = \text{Dirichlet} \left\{ \left(\gamma_1^{(r)}, \dots, \gamma_K^{(r)} \right) \right\}$ where $\gamma_k^{(r)}$ is defined as:

$$\gamma_k^{(r)} = \delta_\pi \left(\gamma_k^{(r-1)} - 1 \right) + \delta_z \sum_{i \in \mathcal{V}} \tau_{ik}^{(r)} + 1. \quad (3.9)$$

Here $\psi(\cdot)$ is the digamma function. Note that the parameters $\tau_{ik}^{(r)}$, $i \in \mathcal{V}$, $k \in \mathcal{K}$, are jointly optimised via a fixed point solver for (3.8), iteratively moving through the rows of the matrix $\tau = \{\tau_{ik}\}_{i \in \mathcal{V}, k \in \mathcal{K}} \in [0, 1]^{N \times K}$ until convergence. The fixed point solver is initialised at the r -th time step by using the value of τ outputted from the $(r-1)$ -th time step as the starting point, which also partially circumvents the problem of label switching (Jasra et al., 2005).

Algorithm 1 describes the full inference procedure based upon the updates in equations (3.7)–(3.9).

3.4 Detecting changepoints

In this work, we aim to detect two types of changepoints: changes in the point process rates and changes in the group memberships.

To detect changes in the point process rates, we compute the KL-divergence between the approximate posteriors $\hat{q}^{(r)}(\lambda_{km})$ and $\hat{q}^{(r-s)}(\lambda_{km})$, for $s = 1, 2, \dots, \kappa$, where $\kappa \in \mathbb{N}$ is a lag parameter. We compare the current approximation with estimates beyond that of the previous update, up to a maximal lag of κ , to avoid

Algorithm 1 Online VB Procedure for BHPP

```

1: Initialise  $\alpha^{(0)}, \beta^{(0)}, \gamma^{(0)}$  and set  $\tau_{ik} = 1/K$  for all  $i \in \mathcal{V}$  and  $k \in \mathcal{K}$ .
2: for  $r = 1, 2, \dots$  do
3:   for  $\ell = 1, 2, \dots, N_{\text{CAVI}}$  do
4:     while  $\tau$  not converged do
5:       for  $j = 1$  to  $N$  do
6:         Update  $\tau_j = (\tau_{j1}, \dots, \tau_{jK})$  as in equation (3.8), initialising as the output of update  $r - 1$ .
7:         Normalise  $\tau_j$  such that  $\sum_{k=1}^K \tau_{jk} = 1$ .
8:       end for
9:     end while
10:    Update  $\gamma^{(r)}, \alpha^{(r)}$  and  $\beta^{(r)}$  as in (3.7)–(3.9).
11:  end for
12: end for
    
```

incorrectly flagging outliers as changes. Figure 6 illustrates the behaviour of the KL-divergence for a lag of 1 and a lag of 2. In Figure 6b, we see that using only a lag of 1 would result in the false identification of a change. There is a trade-off to be made between confidence and speed of detection. We found that a maximal lag of $\kappa = 2$ provided a good balance.

To compute the KL-divergence, we note that $\hat{q}^{(r)}(\lambda_{km})$ is gamma distributed for all $r \in \mathbb{N}$. For two random variables $X_1 \sim \text{Gamma}(\alpha_1, \beta_1)$ and $X_2 \sim \text{Gamma}(\alpha_2, \beta_2)$ with probability distributions p_1 and p_2 respectively, their KL-divergence is:

$$\text{KL}(p_1 \parallel p_2) = \alpha_2 \log \frac{\beta_1}{\beta_2} - \log \frac{\Gamma(\alpha_1)}{\Gamma(\alpha_2)} + (\alpha_1 - \alpha_2)\psi(\alpha_1) - (\beta_1 - \beta_2)\frac{\alpha_1}{\beta_1}.$$

Two burn-in times are required to make use of the KL-divergence. In particular, $B_1 \in \mathbb{N}$ time steps are needed for the algorithm to converge from initialisation, which are then discarded. $B_2 \in \mathbb{N}$ further time steps are needed to obtain enough samples to flag changes. During the initial $B_1 + B_2$ time steps, stationarity is assumed, which is a standard and necessary assumption (see, for example, Bodenhams and Adams (2017)). After $B_1 + B_2$ time steps, we propose to use the median absolute deviation (MAD) to evaluate the presence of a changepoint, as it is robust to outliers (Leys et al., 2013). In general, for a dataset $\mathcal{Y} := \{y_i\}_{i=1}^n$, the MAD is defined as

$$\text{MAD} = \text{med}(\{|y_i - \text{med}(\mathcal{Y})|\}_{i=1}^n),$$

where $\text{med}(\cdot)$ denotes the median of the elements in a set. An observation $y_j \in \mathcal{Y}$ is classified as an outlier if $|y_j - \text{med}(\mathcal{Y})| > W \cdot \text{MAD}$, for a choice of threshold $W \in \mathbb{R}_+$. After a change is flagged, only a further B_2 time steps are required to collect a new dataset for flagging changes from this new state.

In our proposed methodology, the elements in the set \mathcal{Y} are the realised values of the KL-divergence between different gamma distributions, approximating the posterior distributions for the parameters λ_{km} , $k, m \in \mathcal{K}$ at different time windows. For each pair $(k, m) \in \mathcal{K} \times \mathcal{K}$, we let \mathcal{X}_{km}^r store the samples used to check for a changepoint at time step r . For $r = B_1 + B_2 + 1$, define

$$\mathcal{X}_{km}^r := \left\{ p_{km}^{r,1}, \dots, p_{km}^{r,B_2} : p_{km}^{r,\ell} = q^{(B_1+\ell)}(\lambda_{km}) \text{ for } \ell = 1, \dots, B_2 \right\}.$$

We then construct a set of KL-divergences $\mathcal{Y}_{km}^{r,\kappa}$ as

$$\mathcal{Y}_{km}^{r,\kappa} := \left\{ \text{KL} \left[p_{km}^{r,\ell} \parallel p_{km}^{r,\ell-s} \right] : 1 \leq s \leq \kappa, s+1 \leq \ell \leq B_2 \right\}.$$

We then flag $r > B_1 + B_2$ as an outlier if

$$\left| \text{KL} \left[q^{(r)}(\lambda_{km}) \parallel p_{km}^{r,B_2} \right] - \text{med}(\mathcal{Y}_{km}^{r,\kappa}) \right| > W \cdot \text{MAD}.$$

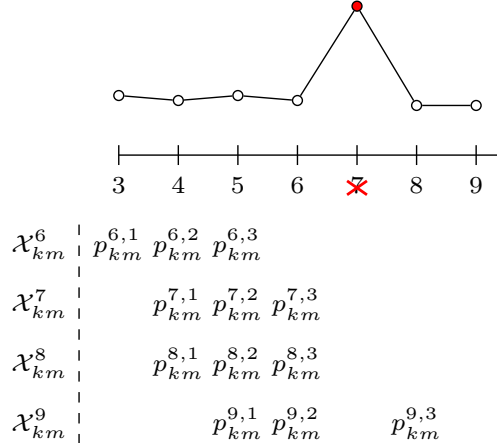


Figure 5: An illustration of how \mathcal{X}_{km}^r is updated for a stream with an outlier at $r = 7$.

If $q^{(r)}(\lambda_{km})$ is not an outlier, we define \mathcal{X}_{km}^{r+1} as

$$\mathcal{X}_{km}^{r+1} := \left\{ p_{km}^{r+1,1}, \dots, p_{km}^{r+1,B_2} : p_{km}^{r+1,\ell-1} = p_{km}^{r,\ell} \text{ for } 2 \leq \ell \leq B_2, \text{ and } p_{km}^{r+1,B_2} = q^{(r)}(\lambda_{km}) \right\},$$

otherwise, we set $\mathcal{X}_{km}^{r+1} = \mathcal{X}_{km}^r$. This update procedure is illustrated in Figure 5. A changepoint is then flagged at update r if κ sequential outliers are detected under this procedure. If a changepoint is detected at r^* , under the assumption of a subsequent B_2 time steps of stationarity, we define

$$\mathcal{X}_{km}^{r^*+B_2} := \left\{ p_{km}^{r^*+B_2,1}, \dots, p_{km}^{r^*+B_2,B_2} : p_{km}^{r^*+B_2,\ell} = q^{(r^*+\ell)}(\lambda_{km}), \ell = 1, \dots, B_2 \right\},$$

and the above procedure is repeated.

We now provide an argument for why the stream must be reset post-change. Suppose a change to the latent rate λ occurs at some time $L_r < t' < L_{r+1}$, and that pre-change $\lambda \sim \text{Gamma}(\alpha, \beta)$, whereas $\lambda \sim \text{Gamma}(\alpha', \beta')$ post-change, for $\alpha \neq \alpha'$ and $\beta \neq \beta'$. Pre-change, our algorithm provides two consecutive CAVI estimates $q^{(r-1)}(\lambda)$ and $q^{(r)}(\lambda)$, with shapes and rates $\alpha^{(r-1)}, \beta^{(r-1)}$ and $\alpha^{(r)}, \beta^{(r)}$, respectively, and post-change, we have CAVI estimates $q^{(r+1)}(\lambda)$ and $q^{(r+2)}(\lambda)$ with shapes and rates $\alpha^{(r+1)}, \beta^{(r+1)}$ and $\alpha^{(r+2)}, \beta^{(r+2)}$. For ease of analysis, we suppose that $\alpha^{(r)} - \alpha^{(r-1)} = \alpha^{(r+2)} - \alpha^{(r+1)} = \Delta_\alpha$, and $\beta^{(r)} - \beta^{(r-1)} = \beta^{(r+2)} - \beta^{(r+1)} = \Delta_\beta$.

We consider the ratio of the KL-divergences between consecutive estimates pre and post-change, and expand as $\Delta_\alpha \rightarrow 0$ to get

$$\frac{\text{KL}(q^{(r+2)} \parallel q^{(r+1)})}{\text{KL}(q^{(r)} \parallel q^{(r-1)})} = \frac{\alpha^{(r+1)} (\Delta_\beta / \beta^{(r+1)} - \log(1 + \Delta_\beta / \beta^{(r+1)}))}{\alpha^{(r-1)} (\Delta_\beta / \beta^{(r-1)} - \log(1 + \Delta_\beta / \beta^{(r-1)}))} \mathcal{O}(\Delta_\alpha). \quad (3.10)$$

Similarly, taking $\Delta_\beta \rightarrow 0$ yields

$$\frac{\text{KL}(q^{(r+2)} \parallel q^{(r+1)})}{\text{KL}(q^{(r)} \parallel q^{(r-1)})} = \frac{\log \{ \Gamma(\alpha^{(r+1)}) / \Gamma(\alpha^{(r+1)} + \Delta_\alpha) \} + \Delta_\alpha \psi(\alpha^{(r+1)})}{\log \{ \Gamma(\alpha^{(r-1)}) / \Gamma(\alpha^{(r-1)} + \Delta_\alpha) \} + \Delta_\alpha \psi(\alpha^{(r-1)})} + \mathcal{O}(\Delta_\beta). \quad (3.11)$$

Observation of (3.10) indicates that to first order the ratio depends upon only the relative size of the difference between their rates, that is Δ_β / β , and not directly upon the magnitude of β . This is not problematic only if the magnitude of Δ_β changes linearly with β . Also, (3.11) shows that the ratio depends directly on the magnitude of the scale α . It follows that after the identification of a changepoint at $t = r_c \Delta$, $r_c \in \mathbb{N}$, the stream of realised KL-divergence values must be discarded, and the algorithm wait a further B_2 time steps to obtain enough samples for the new set $\mathcal{Y}_{km}^s := \{y_{km}^{r,s}\}_{r \geq r_c + B_2 + s}$ which is used to detect any subsequent changes. A further benefit of consider a maximal lag $\kappa > 1$ is that more KL-divergence samples are obtained for the same number of observations.

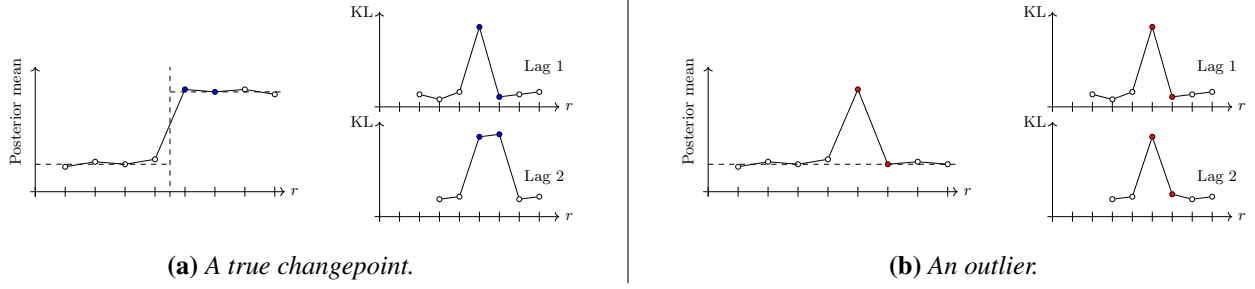


Figure 6: Illustration of the behaviour of the KL-divergence with different lags for a changepoint and an outlier.

To detect changes in the group memberships, the approximation $\prod_{i \in \mathcal{V}} \hat{q}(z_i)$ to the posterior of the latent group memberships in (3.8) provides a node-level vector τ_i ($i = 1, \dots, N$) of group membership probabilities. Computing $\arg\max_k \tau_{ik}$ provides a group assignment for node i , and by comparing assignments between runs, one has a natural way of flagging changes. However, this approach is unsatisfactory as it does not account for the magnitude of the change in probability. The KL-divergence also cannot be used for flagging group changes, since $\text{KL}(p_1 \parallel p_2)$ is only defined only when $p_2 > 0$ for all values in the support of p_1 . Instead, we utilise the Jensen-Shannon divergence (JS; Lin, 1991), defined for two distributions p_1, p_2 as

$$\text{JS}(p_1 \parallel p_2) = \frac{1}{2} \text{KL}(p_1 \parallel p) + \frac{1}{2} \text{KL}(p_2 \parallel p),$$

where $p := (p_1 + p_2)/2$ is a 50-50 mixture distribution of p_1 and p_2 . The JS-divergence is symmetric in its arguments, and avoids the undefined values encountered with the KL-divergence. For $q_1, q_2 \in \Delta^n$, where Δ^n denotes the n -dimensional simplex, the JS-divergence between discrete random variables $X_1 \sim \text{Categorical}(q_1)$ and $X_2 \sim \text{Categorical}(q_2)$, with probability mass functions p_1 and p_2 respectively, takes the following form:

$$\text{JS}(p_1 \parallel p_2) = \frac{1}{2} \left(\sum_{i=1}^n q_{1i} \log \frac{q_{1i}}{(q_{1i} + q_{2i})/2} + \sum_{i=1}^n q_{2i} \log \frac{q_{2i}}{(q_{1i} + q_{2i})/2} \right).$$

The MAD is then used to detect changes to the stream of logged values, in an analogous way to the latent rates, but with two additional requirements on the group probabilities:

$$\arg\max_k \tau_{ik}^{(r)} \neq \arg\max_k \tau_{ik}^{(r-s)}, \quad \text{for all } s = 1, \dots, \kappa, \quad (3.12)$$

$$\arg\max_k \tau_{ik}^{(r-s_1)} = \arg\max_k \tau_{ik}^{(r-s_2)}, \quad \text{for all } s_1, s_2 \in \{1, \dots, \kappa\}. \quad (3.13)$$

If the MAD condition and both (3.12) and (3.13) are met, then a changepoint is flagged. The conditions (3.12) and (3.13) ensure that changes are flagged only if the most likely group assignment changes after a window of κ time steps where the most likely group assignment was stable. It should be noted that for this stream, as the probabilities are constrained to sum to 1, we do not reset these values after a changepoint is detected.

Initialisation of the approximate posterior parameters at update r as the values obtained from update $r - 1$ is a heuristic approach to avoid label switching that we demonstrate works well. An alternative approach would be to instead consider the set of permutations S_K of $[K]$. At each update, one could minimise the KL/JS-divergence over all $\sigma \in S_K$, which would identify the relevant permutation should a label switch have occurred. This would correspond to calculating $\min_{\sigma \in S_K} \text{KL}[q^{(r)}(\lambda_{km}) \parallel p_{\sigma(k)\sigma(m)}^{r, B_2}]$ and identify whether there has been label switching from that. However, such an approach to provide additional robustness would require $\mathcal{O}(K!)$ computations, which could be undesirable for an online algorithm.

Note that identifiability issues may arise in the case that a rate and membership change occur simultaneously. However, in simulations conducted with a small proportion of nodes changing groups ($\approx 25\%$) at the same time as a change to the latent rates, no identifiability issues were encountered.

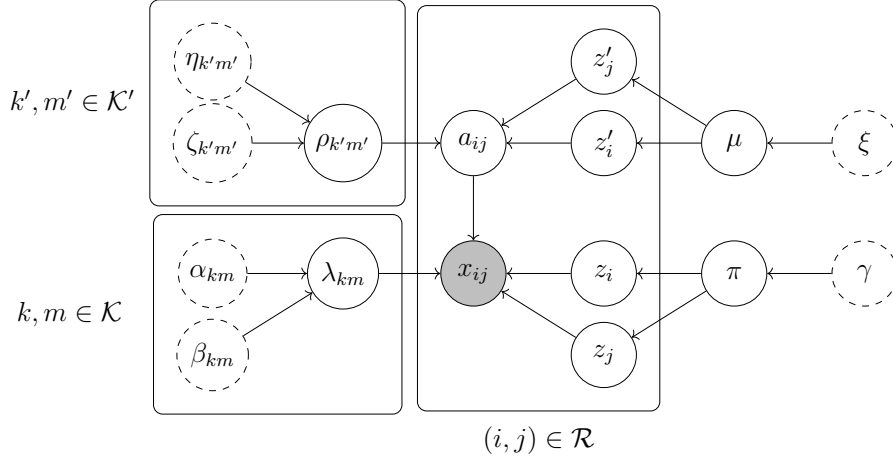


Figure 7: A directed acyclic graphical model representation of the model in (3.14)-(3.16).

3.5 Online VB for the dynamic BHPP with an unknown underlying graph

Until now, it has been assumed that the graph is fully connected. We relax this assumption and extend the framework to the setting where $\mathbf{A} = \{a_{ij}\} \in \{0, 1\}^{N \times N}$ is unknown. Assuming $a_{ij} = 1$ when there is no edge adversely affects estimation of the latent rates; instead of the absence of an event indicating the absence of an edge, it instead just leads to a lower rate estimate. This motivates a method that can take into account the possibility that $a_{ij} = 0$. The work here builds upon the sparse setup of [Matias et al. \(2018\)](#).

For each $(i, j) \in \mathcal{R}$, an additional latent variable $a_{ij} \in \{0, 1\}$ is introduced. A new latent group membership $z'_i \in \mathcal{K}' := \{1, \dots, K'\}$ is assigned to each $i \in \mathcal{V}$, and a_{ij} is Bernoulli-distributed conditional upon z'_i and z'_j , according to a stochastic blockmodel (SBM; [Holland et al., 1983](#)). Each a_{ij} captures the probability that $(i, j) \in \mathcal{R}$ is also an element of \mathcal{E} , and functions to reduce the contribution of edges with no arrivals to the estimates of the underlying rates. The new model is then expressed as:

$$x_{ij}(t) \mid a_{ij}, z_i, z_j, \lambda_{z_i z_j} \sim \text{Poisson}(a_{ij} \lambda_{z_i z_j} t), \quad \text{for all } i, j \in \mathcal{V}, \quad (3.14)$$

$$\lambda_{km} \sim \text{Gamma}(\alpha_{km}^0, \beta_{km}^0), \quad \text{for all } k, m \in \mathcal{K},$$

$$a_{ij} \mid z'_i, z'_j, \rho_{z'_i z'_j} \sim \text{Bernoulli}(\rho_{z'_i z'_j}), \quad \text{for all } i, j \in \mathcal{V},$$

$$\rho_{k'm'} \sim \text{Beta}(\eta_{k'm'}^0, \zeta_{k'm'}^0), \quad \text{for all } k', m' \in \mathcal{K}',$$

$$z_i \mid \pi \sim \text{Categorical}(\pi), \quad \text{for all } i \in \mathcal{V},$$

$$z'_i \mid \mu \sim \text{Categorical}(\mu), \quad \text{for all } i \in \mathcal{V},$$

$$\pi \sim \text{Dirichlet}(\gamma^0), \quad (3.15)$$

$$\mu \sim \text{Dirichlet}(\xi^0), \quad (3.16)$$

We refer to this model as the stochastic blockmodel BHPP (SBM-BHPP). We allow the most general setting in which the group structure that governs the rates is separate from that which determines edge connection probabilities. We assume that the graph is static, and so changes to the memberships that drive the edge-processes should not affect the determination of the graph adjacency matrix. The decoupling of the edge-process and edge-connection group memberships ensure this. Furthermore, as has been noted, SBMs provide good approximations to any exchangeable random graph model ([Airoldi et al., 2013](#)), and they therefore offer a logical model for the graph generation mechanism. This new model structure is represented in graphical model form in Figure 7.

Given the graph is considered to be static, if $x_{ij}(t) > 0$ for some t , then $(i, j) \in \mathcal{E}$ (corresponding to $a_{ij} = 1$) with probability one. Otherwise, if $x_{ij}(t) = 0$ then we either have no edge (corresponding to $a_{ij} = 0$), or a non-null intensity process with no events in $(0, t]$. The difference with the Section 2.1 is that we now have the additional local latent variables, z, z' and \mathbf{A} , all of which grow with N (linearly for z and z' , and quadratically for \mathbf{A}).

To implement variational inference, the full conditional distribution $p(a_{ij} \mid z_i, z_j, z'_i, z'_j, \lambda_{z_i z_j}, \rho_{z'_i z'_j}, \mathcal{D}_{1:r})$ must be written down exactly, as per (3.3). Using the fact that inter-arrival times from a Poisson process are exponentially distributed, Matias et al. (2018) shows that the conditional posterior probability of an edge $(i, j) \in \mathcal{E}$ in the case of static λ takes the form

$$p(a_{ij} = 1 \mid \mathcal{D}_{1:r}, z_i = k, z_j = m, z'_i = k', z'_j = m', \lambda_{km}, \rho_{k'm'}) = \mathbb{I}\{x_{ij}(r\Delta) > 0\} + \frac{\mathbb{I}\{x_{ij}(r\Delta) = 0\} \rho_{k'm'} \exp(-\lambda_{km} r \Delta)}{1 - \rho_{k'm'} + \rho_{k'm'} \exp(-\lambda_{km} r \Delta)}. \quad (3.17)$$

Since \mathbf{A} is static, the posterior for each a_{ij} should be computed using the full data $\mathcal{D}_{1:r}$. Note that the conditional distribution in (3.17) depends on $\mathcal{D}_{1:r}$ only via the counting process $x_{ij}(\cdot)$ at time $r\Delta$. For the model in (3.14)-(3.16), the true posterior distribution after r batches factorises as

$$p(\mathbf{A}, z, z', \theta \mid \mathcal{D}_{1:r}) \propto p(\mathcal{D}_r \mid \mathbf{A}, z, z', \theta) \times p(\mathbf{A}, z, z', \theta \mid \mathcal{D}_{1:(r-1)}),$$

similarly to the posterior distribution in (3.4). Therefore, inference on this model can be performed in much the same way as inference on the original model. However, as the true conditional posterior for \mathbf{A} is tractable, the update procedure is slightly different. Unlike Matias et al. (2018), we cannot simply take $q^{(r)}(a_{ij})$ to be Bernoulli distributed with probability as in (3.17) as λ is, in general, not static. Instead, to account for variations in λ over the full observation window, we propose an approximation to the posterior distribution of a_{ij} at $t = r\Delta$, conditional upon $z_i = k, z_j = m, z'_i = k', z'_j = m'$, of the form $\hat{q}^{(r)}(a_{ij}) = \text{Bernoulli}(\sigma_{ij}^{(r)})$, where

$$\sigma_{ij}^{(r)} = \mathbb{I}\{x_{ij}(r\Delta) > 0\} + \frac{\mathbb{I}\{x_{ij}(r\Delta) = 0\} \hat{\rho}_{k'm'}^{(r)} \exp\left(-\Delta \sum_{\ell=0}^r \hat{\lambda}_{km}^{(\ell)}\right)}{1 - \hat{\rho}_{k'm'}^{(r)} + \hat{\rho}_{k'm'}^{(r)} \exp\left(-\Delta \sum_{\ell=0}^r \hat{\lambda}_{km}^{(\ell)}\right)}. \quad (3.18)$$

Here, $\hat{\rho}_{k'm'}^{(\ell)}$ and $\hat{\lambda}_{km}^{(\ell)}$ denote the mean of our approximate posterior distribution for $\rho_{k'm'}$ and λ_{km} , respectively, at update ℓ . At update r , we propose a variational approximation of the form $q^{(r)}(\mathbf{A}, z, z', \theta) = \prod_{(i,j) \in \mathcal{R}} \text{Bernoulli}(\sigma_{ij}^{(r)}) \times q(\theta, z, z')$, where $\sigma_{ij}^{(r)}$ is as in (3.18) and $q(\theta, z, z') \in \mathcal{F}^{2N+S}$. A two-step estimation procedure follows naturally, wherein $q(\theta, z, z')$ is approximated using CAVI as was done previously, and then $\sigma_{ij}^{(r)}$ is updated using (3.18) and the CAVI approximations to the posteriors of λ and ρ .

Note that since a_{ij} for $i, j \in \mathcal{V}$, z'_i for $i \in \mathcal{V}$, $\rho_{k'm'}$ for $k', m' \in \mathcal{K}'$ and μ are considered *static* parameters, forgetting factors for these quantities are not required.

Consider the BHPP model with unknown graph structure, as in (3.14)-(3.16), with global parameters $\theta = (\lambda, \pi, \mu, \rho)$ and local parameters z, z' and \mathbf{A} . At step $r - 1$, we approximate the posterior density $p(\mathbf{A}, z, z', \theta \mid \mathcal{D}_{1:(r-1)})$ by $\hat{q}^{(r-1)}(\mathbf{A}, z, z', \theta)$, which is the product of the optimal CAVI solution $\hat{q}^{(r-1)}(z, z', \theta)$ and the fixed-form approximation $\hat{q}^{(r-1)}(\mathbf{A})$ of (3.18). For the BHPP model with known graph structure, all latent variables could change, and thus in (3.6) all components were tempered before being passed as the prior for time steps r . However, in the case of an unknown graph structure, as the graph is assumed to be static, only the components of the dynamic latent variables are tempered when constructing the prior for time step r . We pass through as the prior for time step r the partially tempered density

$$\begin{aligned} \hat{q}_{\delta}^{(r-1)}(\mathbf{A}, z, \theta) &= \prod_{k, m \in \mathcal{K}} \hat{q}^{(r-1)}(\rho_{km}) \times \prod_{i \in \mathcal{V}} \hat{q}^{(r-1)}(z'_i) \times \prod_{(i, j) \in \mathcal{R}} \hat{q}^{(r-1)}(a_{ij}) \times \hat{q}^{(r-1)}(\mu) \\ &\times \prod_{i \in \mathcal{V}} \hat{q}_{\delta_z}^{(r-1)}(z_i) \times \prod_{k, m \in \mathcal{K}} \hat{q}_{\delta_\lambda}^{(r-1)}(\lambda_{km}) \times \hat{q}_{\delta_\pi}^{(r-1)}(\pi). \end{aligned} \quad (3.19)$$

We assume that each component of (3.19) takes the same form as its corresponding complete conditional distribution under the BHPP model with unknown graph structure of (3.14)-(3.16). Additionally, the distributions for λ, π and z are raised to a power and normalised. In summary:

$$\hat{q}^{(r-1)}(a_{ij}) = \text{Bernoulli}\left(\sigma_{ij}^{(r-1)}\right), \quad \text{for all } i, j \in \mathcal{V},$$

$$\begin{aligned}
 \hat{q}_{\delta_\lambda}^{(r-1)}(\lambda_{km}) &= \frac{1}{C_{\lambda_{km}, r-1}} \text{Gamma} \left(\alpha_{km}^{(r-1)}, \beta_{km}^{(r-1)} \right)^{\delta_\lambda}, & \text{for all } k, m \in \mathcal{K}, \\
 \hat{q}^{(r-1)}(\rho_{k'm'}) &= \text{Beta} \left(\eta_{k'm'}^{(r-1)}, \zeta_{k'm'}^{(r-1)} \right), & \text{for all } k', m' \in \mathcal{K}', \\
 \hat{q}^{(r-1)}(z_i) &= \frac{1}{C_{z_i, r-1}} \text{Categorical} \left(\tau_i^{(r-1)} \right)^{\delta_z}, & \text{for all } i \in \mathcal{V}, \\
 \hat{q}^{(r-1)}(z'_i) &= \text{Categorical} \left(\nu_i^{(r-1)} \right), & \text{for all } i \in \mathcal{V}, \\
 \hat{q}_{\delta_\pi}^{(r-1)}(\pi) &= \frac{1}{C_{\pi, r-1}} \text{Dirichlet} \left(\gamma^{(r-1)} \right)^{\delta_\pi}, \\
 \hat{q}^{(r-1)}(\mu) &= \text{Dirichlet} \left(\xi^{(r-1)} \right).
 \end{aligned}$$

Suppose that data is again observed on the interval $I_r := (L_{r-1}, L_r]$, for $r \in \mathbb{N}$. Under the prior structure in (3.19), the CAVI sequential updates take the form:

1. $\hat{q}^{(r)}(\lambda_{km}) = \text{Gamma} \left(\alpha_{km}^{(r)}, \beta_{km}^{(r)} \right)$ where for all $k, m \in \mathcal{K}$ we define $\alpha_{km}^{(r)}$ and $\beta_{km}^{(r)}$ as

$$\begin{aligned}
 \alpha_{km}^{(r)} &= \delta_\lambda \left(\alpha_{km}^{(r-1)} - 1 \right) + \sum_{(i,j) \in \mathcal{R}} \tau_{ik}^{(r-1)} \tau_{jm}^{(r-1)} \sigma_{ij}^{(r-1)} x_{ij}^{(r)} + 1, \\
 \beta_{km}^{(r)} &= \delta_\lambda \beta_{km}^{(r-1)} + \sum_{(i,j) \in \mathcal{R}} \tau_{ik}^{(r-1)} \tau_{jm}^{(r-1)} \sigma_{ij}^{(r-1)}.
 \end{aligned}$$

2. $\hat{q}^{(r)}(\rho_{k'm'}) = \text{Beta} \left(\eta_{k'm'}^{(r)}, \zeta_{k'm'}^{(r)} \right)$ where for all $k', m' \in \mathcal{K}'$, we define $\eta_{k'm'}^{(r)}$ and $\zeta_{k'm'}^{(r)}$ as

$$\begin{aligned}
 \eta_{k'm'}^{(r)} &= \eta_{k'm'}^{(r-1)} + \sum_{(i,j) \in \mathcal{R}} \nu_{ik'}^{(r-1)} \nu_{jm'}^{(r-1)} \sigma_{ij}^{(r-1)} + 1, \\
 \zeta_{k'm'}^{(r)} &= \zeta_{k'm'}^{(r-1)} + \sum_{(i,j) \in \mathcal{R}} \nu_{ik'}^{(r-1)} \nu_{jm'}^{(r-1)} \left(1 - \sigma_{ij}^{(r-1)} \right).
 \end{aligned}$$

3. $\hat{q}^{(r)}(z_i) = \text{Categorical} \left(\tau_i^{(r)} \right)$ for all $i \in \mathcal{V}$ where $\tau_i^{(r)} = (\tau_{i1}^{(r)}, \dots, \tau_{iK}^{(r)})$, with $\sum_{k \in \mathcal{K}} \tau_{ik}^{(r)} = 1$, satisfies the relation:

$$\begin{aligned}
 \tau_{ik}^{(r)} &\propto \exp \left\{ \delta_z \left[\psi \left(\gamma_k^{(r-1)} \right) - \psi \left(\sum_{\ell=1}^K \gamma_\ell^{(r-1)} \right) \right] + \sum_{j \in \mathcal{V}} \sum_{m \in \mathcal{K}} \tau_{jm}^{(r)} \left(1 - \mathbb{I}_{\{i\}}(j) \mathbb{I}_{\{k\}}(m) \right) \right. \\
 &\quad \times \left[-\Delta \left(\sigma_{ij}^{(r-1)} \frac{\alpha_{km}^{(r)}}{\beta_{km}^{(r)}} + \sigma_{ji}^{(r-1)} \frac{\alpha_{mk}^{(r)}}{\beta_{mk}^{(r)}} \right) + x_{ij}(I_r) \sigma_{ij}^{(r-1)} \left(\psi \left(\alpha_{km}^{(r)} \right) - \log \left(\beta_{km}^{(r)} \right) \right) \right. \\
 &\quad \left. \left. + x_{ji}(I_r) \sigma_{ji}^{(r-1)} \left(\psi \left(\alpha_{mk}^{(r)} \right) - \log \left(\beta_{mk}^{(r)} \right) \right) \right] + \sigma_{ii}^{(r-1)} \left[x_{ii}(I_r) \left(\psi \left(\alpha_{kk}^{(r)} \right) - \log \left(\beta_{kk}^{(r)} \right) \right) \right. \right. \\
 &\quad \left. \left. - \Delta \frac{\alpha_{kk}^{(r)}}{\beta_{kk}^{(r)}} \right] \right\}.
 \end{aligned}$$

4. $\hat{q}^{(r)}(z'_i) = \text{Categorical} \left(\nu_i^{(r)} \right)$ for all $i \in \mathcal{V}$ where $\nu_i^{(r)} = (\nu_{i1}^{(r)}, \dots, \nu_{iK'}^{(r)})$, with $\sum_{k' \in \mathcal{K}'} \nu_{ik'}^{(r)} = 1$, satisfies the relation:

$$\nu_{ik'}^{(r)} \propto \exp \left\{ \psi \left(\xi_{k'}^{(r)} \right) - \psi \left(\sum_{\ell'=1}^{K'} \xi_{\ell'}^{(r)} \right) + \sum_{j \in \mathcal{V}} \sum_{m' \in \mathcal{K}'} \nu_{jm'}^{(r)} \left(1 - \mathbb{I}_{\{k'\}}(m') \mathbb{I}_{\{i\}}(j) \right) \right\}$$

$$\begin{aligned} & \times \left[\sigma_{ij}^{(r)} \left(\psi \left(\eta_{k'm'}^{(r)} \right) - \psi \left(\eta_{k'm'}^{(r)} + \zeta_{k'm'}^{(r)} \right) \right) + \left(1 - \sigma_{ij}^{(r)} \right) \left(\psi \left(\zeta_{k'm'}^{(r)} \right) - \psi \left(\zeta_{k'm'}^{(r)} + \eta_{k'm'}^{(r)} \right) \right) \right. \\ & \left. + \sigma_{ji}^{(r)} \left(\psi \left(\eta_{m'k'}^{(r)} \right) - \psi \left(\eta_{m'k'}^{(r)} + \zeta_{m'k'}^{(r)} \right) \right) + \left(1 - \sigma_{ji}^{(r)} \right) \left(\psi \left(\zeta_{m'k'}^{(r)} \right) - \psi \left(\zeta_{m'k'}^{(r)} + \eta_{m'k'}^{(r)} \right) \right) \right] \\ & + \sigma_{ii}^{(r)} \left[\psi \left(\eta_{k'k'}^{(r)} \right) - \psi \left(\eta_{k'k'}^{(r)} + \zeta_{k'k'}^{(r)} \right) \right] + \left(1 - \sigma_{ii}^{(r)} \right) \left(\psi \left(\zeta_{k'k'}^{(r)} \right) - \psi \left(\eta_{k'k'}^{(r)} + \zeta_{k'k'}^{(r)} \right) \right) \Big\}. \end{aligned}$$

5. $\hat{q}^{(r)}(\pi) = \text{Dirichlet}(\gamma^{(r)})$ where for all $k \in \mathcal{K}$, we define $\gamma_k^{(r)}$ as:

$$\gamma_k^{(r)} = \delta_\pi \left(\gamma_k^{(r-1)} - 1 \right) + \delta_z \sum_{i \in \mathcal{V}} \tau_{ik}^{(r)} + 1.$$

6. $\hat{q}^{(r)}(\mu) = \text{Dirichlet}(\xi^{(r)})$ where for all $k' \in \mathcal{K}'$, we define $\xi_{k'}^{(r)}$ as:

$$\xi_{k'}^{(r)} = \xi_{k'}^{(r-1)} + \sum_{i \in \mathcal{V}} \nu_{ik'}^{(r)}.$$

7. $\hat{q}^{(r)}(a_{ij}) = \text{Bernoulli}(\sigma_{ij}^{(r)})$, where $\sigma_{ij}^{(r)}$ is defined in (3.18) for all $i, j \in \mathcal{V}$.

3.6 Online VB for the dynamic BHPP with an unknown number of groups

In real-world applications, the number of groups K is usually unknown, and it must be estimated from the observed data. To address this issue, we adopt a Bayesian non-parametric approach, proposing a Dirichlet process prior (Ferguson, 1973) on the group memberships. In particular, we replace the Dirichlet prior distributions in (2.3) and (3.15) with a Griffiths-Engen-McCloskey (GEM; Pitman, 2002) prior distribution, with parameter ν , written $\pi \sim \text{GEM}(\nu)$. This prior distribution corresponds to an infinite limit of a Dirichlet distribution: $\text{GEM}(\nu) = \lim_{K \rightarrow \infty} \text{Dirichlet}(\nu \mathbf{1}_K / K)$, where $\mathbf{1}_K$ is the vector of ones of length K . The full model becomes:

$$x_{ij}(t) \mid z_i, z_j, \lambda_{z_i z_j} \sim \text{Poisson}(\lambda_{z_i z_j} t), \quad \text{for all } (i, j) \in \mathcal{E}, \quad (3.20)$$

$$\lambda_{km} \sim \text{Gamma}(\alpha, \beta), \quad \text{for all } k, m \in \mathbb{N},$$

$$z_i \mid \pi \sim \text{Categorical}(\pi), \quad \text{for all } i \in \mathcal{V},$$

$$\pi \sim \text{GEM}(\nu), \quad (3.21)$$

where π represents an infinite sequence π_1, π_2, \dots such that $\pi_k \geq 0$ for all $k = 1, 2, \dots$ and $\sum_{k=1}^{\infty} \pi_k = 1$. The GEM prior distribution also corresponds to the distribution of proportions obtained under a stick-breaking representation (Sethuraman, 1994) of a Dirichlet process. Therefore, the proportions π can be reparametrised as a product of variables $u_1, u_2, \dots \in [0, 1]$ drawn from independent beta distributions, as follows:

$$u_k \sim \text{Beta}(1, \nu), \quad \pi_k := u_k \prod_{\ell=1}^{k-1} (1 - u_\ell), \text{ for } k = 1, 2, \dots \quad (3.22)$$

This decomposition is particularly useful to derive an online variational inference algorithm for the BHPP model with GEM priors (GEM-BHPP), following Blei and Jordan (2006). In particular, within a mean-field approximation $q(\lambda, u, z) = q(\lambda) \times q(u) \times q(z)$ for the posterior distribution $p(\lambda, u, z \mid \mathcal{D}_{1:r})$, a variational approximation $q(u) = \prod_{\ell=1}^{\infty} q(u_\ell)$ is posited directly on u_1, u_2, \dots , rather than π . This approximation is truncated at a level $L \in \mathbb{N}$, implying that $q(u_\ell) = \delta_0(u_\ell)$ for $\ell = L + 1, L + 2, \dots$, effectively resulting in an L -dimensional probability vector from (3.22).

It should be pointed out how this approach differs from the model set-up we considered earlier. In the GEM-BHPP, we make no truncation in the model set-up, but rather only in the variational approximation to it.

This is in contrast to the method we presented in Sections 2.1, wherein one would be using a finite-dimensional Dirichlet distribution directly in the prior structure.

We introduce the notation $\omega_i^{(r)}$, $\nu_i^{(r)}$, $\alpha_{km}^{(r)}$ and $\beta_{km}^{(r)}$, for $i, k, m \in \{1, \dots, L\}$. If we define $\omega_i^{(0)} \equiv 1$, $\nu_i^{(0)} \equiv \nu$ for all $i \in \{1, \dots, L\}$ and $\alpha_{km}^{(0)} \equiv \alpha$ and $\beta_{km}^{(0)} \equiv \beta$, for all $k, m \in \{1, \dots, L\}$, the first time step takes the form of the model specified in (3.20)–(3.21). Using this notation, we can formulate our inference procedure based on the same process of sequential CAVI updates.

Consider the GEM-BHPP model in (3.21)–(3.20) with a stick-breaking reparametrisation of π as in 3.22, global parameters $\theta = (\lambda, u)$ and local parameters z . The posterior distribution $p(\theta, z \mid \mathcal{D}_{1:(r-1)})$ is approximated by the optimal CAVI solution $\hat{q}^{(r-1)}(\theta, z)$. Similarly to (3.6), this CAVI approximation is tempered to form $\hat{q}_\delta^{(r-1)}(\theta, z)$, taking the following product form:

$$\hat{q}_\delta^{(r-1)}(\theta, z) = \prod_{k=1}^L \prod_{m=1}^L \hat{q}_{\delta_\lambda}^{(r-1)}(\lambda_{km}) \times \prod_{i \in \mathcal{V}} \hat{q}_{\delta_z}^{(r-1)}(z_i) \times \prod_{\ell=1}^L \hat{q}_{\delta_u}^{(r-1)}(u_\ell). \quad (3.23)$$

This tempered density is then passed through as the prior for time step r . We assume that each component of (3.23) takes the same form of its corresponding complete conditional distribution under the GEM-BHPP model in (3.20)–(3.21), raised to a power and normalised:

$$\begin{aligned} \hat{q}_{\delta_\lambda}^{(r-1)}(\lambda_{km}) &= \frac{1}{C_{\lambda_{km}, r-1}} \text{Gamma} \left(\alpha_{km}^{(r-1)}, \beta_{km}^{(r-1)} \right)^{\delta_\lambda}, & \text{for all } k, m \in \{1, \dots, L\}, \\ \hat{q}_{\delta_z}^{(r-1)}(z_i) &= \frac{1}{C_{z_i, r-1}} \text{Categorical}(\tau^{(r-1)})^{\delta_z}, & \text{for all } i \in \mathcal{V}, \\ \hat{q}_{\delta_u}^{(r-1)}(u_\ell) &= \frac{1}{C_{u_\ell, r-1}} \text{Beta} \left(\omega_\ell^{(r-1)}, \nu_\ell^{(r-1)} \right)^{\delta_u}, & \text{for all } \ell \in \{1, \dots, L\}, \end{aligned}$$

where $C_{\lambda_{km}, r-1}$, $C_{z_i, r-1}$ and $C_{u_\ell, r-1}$ are normalising constants, ensuring that the densities are valid, and $\delta = (\delta_\lambda, \delta_z, \delta_u) \in (0, 1]^3$ are temperature parameters specific to each class of latent variables. Suppose that data is observed on the interval $I_r := (L_{r-1}, L_r]$, for $r \in \mathbb{N}$, and denote the count on edge (i, j) during this interval by $x_{ij}(I_r)$. Under the prior structure in (3.23), the CAVI sequential updates then take the form

1. $\hat{q}^{(r)}(\lambda_{km}) = \text{Gamma}(\alpha_{km}^{(r)}, \beta_{km}^{(r)})$ for all $k, m \in \mathcal{K}$ where $\alpha_{km}^{(r)}, \beta_{km}^{(r)}$ are defined as:

$$\begin{aligned} \alpha_{km}^{(r)} &= \delta_\lambda \left(\alpha_{km}^{(r-1)} - 1 \right) + \sum_{(i,j) \in \mathcal{E}} \tau_{ik}^{(r-1)} \tau_{jm}^{(r-1)} x_{ij}(I_r) + 1, \\ \beta_{km}^{(r)} &= \delta_\lambda \beta_{km}^{(r-1)} + \Delta \sum_{(i,j) \in \mathcal{E}} \tau_{ik}^{(r-1)} \tau_{jm}^{(r-1)}. \end{aligned} \quad (3.24)$$

2. $\hat{q}^{(r)}(z_i) = \text{Categorical}(\tau_i^{(r)})$ for all $i \in \mathcal{V}$ where $\tau_i^{(r)} = (\tau_{i1}^{(r)}, \dots, \tau_{iL}^{(r)})$, with $\sum_{k \in \mathcal{L}} \tau_{ik}^{(r)} = 1$, satisfies the relation:

$$\begin{aligned} \tau_{ik}^{(r)} &\propto \exp \left\{ \delta_z \left[\psi \left(\omega_k^{(r-1)} \right) - \psi \left(\omega_k^{(r-1)} + \nu_k^{(r-1)} \right) + \sum_{\ell=1}^{k-1} \left(\psi \left(\nu_\ell^{(r-1)} \right) - \psi \left(\omega_\ell^{(r-1)} + \nu_\ell^{(r-1)} \right) \right) \right] \right. \\ &\quad + \sum_{m=1}^L \left[\sum_{j: (i,j) \in \mathcal{E}} \tau_{jm}^{(r)} \left(1 - \mathbb{I}_{\{k\}}(m) \mathbb{I}_{\{i\}}(j) \right) \left(x_{ij}(I_r) \left[\psi \left(\alpha_{km}^{(r)} \right) - \log \left(\beta_{km}^{(r)} \right) \right] - \Delta \frac{\alpha_{km}^{(r)}}{\beta_{km}^{(r)}} \right) \right. \\ &\quad + \sum_{j': (j', i) \in \mathcal{E}} \tau_{j'm}^{(r)} \left(1 - \mathbb{I}_{\{k\}}(m) \mathbb{I}_{\{i\}}(j') \right) \left(x_{j'i}(I_r) \left[\psi \left(\alpha_{mk}^{(r)} \right) - \log \left(\beta_{mk}^{(r)} \right) \right] - \Delta \frac{\alpha_{mk}^{(r)}}{\beta_{mk}^{(r)}} \right) \right. \\ &\quad \left. \left. + x_{ii}(I_r) \left[\psi \left(\alpha_{kk}^{(r)} \right) - \log \left(\beta_{kk}^{(r)} \right) \right] - \Delta \frac{\alpha_{kk}^{(r)}}{\beta_{kk}^{(r)}} \right] \right\}. \end{aligned} \quad (3.25)$$

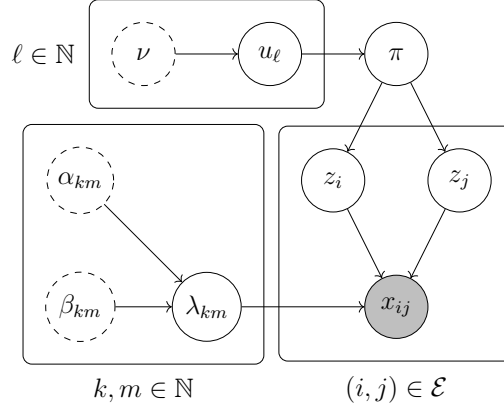


Figure 8: A directed acyclic graph of the model given by (3.20)-(3.21).

3. $\hat{q}^{(r)}(u_i) = \text{Beta}(\omega_i^{(r)}, \nu_i^{(r)})$ for all $i \in \{1, \dots, L\}$ where $\omega_i^{(r)}$ and $\nu_i^{(r)}$ are defined as:

$$\begin{aligned}\omega_i^{(r)} &= \delta_u (\omega_i^{(r-1)} - 1) + \delta_z \sum_{j \in \mathcal{V}} \tau_{ji}^{(r)} + 1, \\ \nu_i^{(r)} &= \delta_u (\nu_i^{(r-1)} - 1) + \delta_z \sum_{j \in \mathcal{V}} \sum_{k=i+1} \tau_{jk}^{(r)} + 1.\end{aligned}$$

A subtle problem arises with the updates in (3.24). In the case that the truncation parameter, L , is larger than the true number of groups, the update procedure will allocate some groups zero nodes. If $\ell \in \{1, \dots, L\}$ is one such group, then for all $i \in \mathcal{V}$ $\tau_{i\ell}^{(r)} = 0$ for every r after the algorithm has converged, up until a change occurs. For $\delta_\lambda \in (0, 1)$, it follows from the rate update in (3.24) that $\lim_{r \rightarrow \infty} \beta_{\ell m}^{(r)} = \lim_{r \rightarrow \infty} \beta_{m\ell}^{(r)} = 0$ for all $m \in \{1, \dots, L\}$, and thus that the posterior mean of $\lambda_{\ell m}$ and $\lambda_{m\ell}$ diverges. This divergence causes problems in (3.25) where this mean appears. To circumvent this problem, we must replace δ_λ with the set $\{\delta_\lambda^{km}\}_{k,m=1}^L$. That is, we introduce a specific forgetting factor for each group-to-group rate. For each, $k, m \in \{1, \dots, L\}$, we initially set $\delta_L^{km} \equiv \delta_\lambda$, but monitor the sum $\sum_{(i,j) \in \mathcal{E}} \tau_{ik}^{(r-1)} \tau_{jm}^{(r-1)}$ with increasing r . Then, for all $k, m \in \{1, \dots, L\}$ such that $\sum_{(i,j) \in \mathcal{E}} \tau_{ik}^{(r-1)} \tau_{jm}^{(r-1)} < \epsilon$, we set $\delta_{km} = 1$, where ϵ is some threshold. This intervention prevents the exponential decay of $\beta_{km}^{(r)}$ to 0 as $r \rightarrow \infty$. Once the threshold is exceeded, the relevant BFFs are returned to δ_λ . Experimentation found that 0.1 is a good choice for ϵ .

4 Simulation studies

We evaluate the online changepoint detection algorithm of Section 3 using simulated data. Five simulation studies are conducted. In Section 4.1, we examine membership and rate recovery in the case that \mathbf{A} and \mathbf{K} are known when a varying proportion of nodes swap between the two groups. In Section 4.2, membership recovery is investigated when \mathbf{A} is known, but \mathbf{K} changes throughout the observation window. In Section 4.3, we consider two the effect of a decreasing lag between two instantaneous changes to λ when both \mathbf{A} and \mathbf{K} are known. In Section 4.4, the effect of increasing sparsity in case of known \mathbf{K} but unknown \mathbf{A} is examined. Finally, in Section 4.5, we examine the recovery of group memberships with varying latent rates.

Unless otherwise stated, we consider a network with $N = 500$ nodes and $K = 2$ latent groups, initialised with $\Pi = (0.6, 0.4)$. For convenience, we define the intra-inter-group rate matrix

$$\lambda_0 = \begin{pmatrix} 2 & 1 \\ 0.3 & 8 \end{pmatrix}. \quad (4.1)$$

The update interval is set to $\Delta = 0.1$ time units throughout, and every experiment is repeated 50 times, with the results averaged. We cycle 3 times over the CAVI and fixed point equations. All hyperparameters are initialised

as 1, except for γ and ξ , which are initialised uniformly on $[0.95, 1.05]^K$ and $[0.95, 1.05]^{K'}$, respectively. For all $i, j \in \mathcal{V}$, σ_{ij} is initialised as $1/2$, and τ_i as $\mathbf{1}_K/K$, when K is known, and as $\mathbf{1}_L/L$ when we infer the number of groups at a truncation level of L . Unless otherwise stated, W_{JS} is set to be 2 and W_{KL} , B_1 and B_2 to 10.

4.1 Latent group membership recovery

The first experiment takes a fully-connected network with rate matrix λ_0 as given in (4.1). At time $t = 3$, $P\%$ of nodes from group 1 swap to group 2, with $P \in \{1, 10, 25, 50, 75, 95\}$. To evaluate latent membership recovery, the inferred group memberships at time t are compared to the true memberships using the adjusted rand index (ARI, [Hubert and Arabie, 1985](#)). The ARI takes values between -1 and 1 , with a value of 1 indicating perfect agreement (up to label switching), 0 random agreement, and -1 complete disagreement. By computing the ARI at each update, rather than taking an average over $[0, t]$, we can examine the smoothness of recovery, and the reaction of the algorithm to changepoints.

Figure 9a shows the inference procedure is stable across all values of P , where the plots begin from B_1 time steps. The ARI is steady before and after the change except for the time step immediately after the change. Figure 9b shows that the algorithm quickly converges to the true proportions, both with and without a BFF. Note that in both figures, the pink and green lines are indistinguishable from one another.

4.2 Number of groups recovery

We consider a fully connected network with two group membership changes: all nodes merging into group 1 at $t = 2.5$, followed by the creation of a new group at $t = 3.5$. We use the GEM-BHPP model for this simulation. Specifically, at $t = 3.5$, $P\%$ of the nodes in group 1 remain, while the remainder create group 2. We again consider $P \in \{1, 10, 25, 50, 75, 95\}$, with λ_0 as the rate matrix, and ARI as our performance metric. We set $W_{JS} = 0$ here, which corresponds to taking the argmax of each τ_i .

Figure 10 shows that the inference correctly groups the nodes in all cases pre-merger and between the merger and creation, both with and without a BFF. Using a BFF, the algorithm is seen to maintain a high ARI after the creation of a new group, in all cases except when $P = 75$. The application without the BFF also fails in this case, but additionally it fails for $P = 50$, and is slower to converge to the new groups when $P = 25$ and 10 .

For cases where 50% of nodes or less remain in group 1, the algorithm converges to the correct proportions, but with label-switching. This is observed in Figure 11, where the rates are seen to swap in the 10% panel for the case of a BFF.

4.3 Detection of changes to the matrix of rates

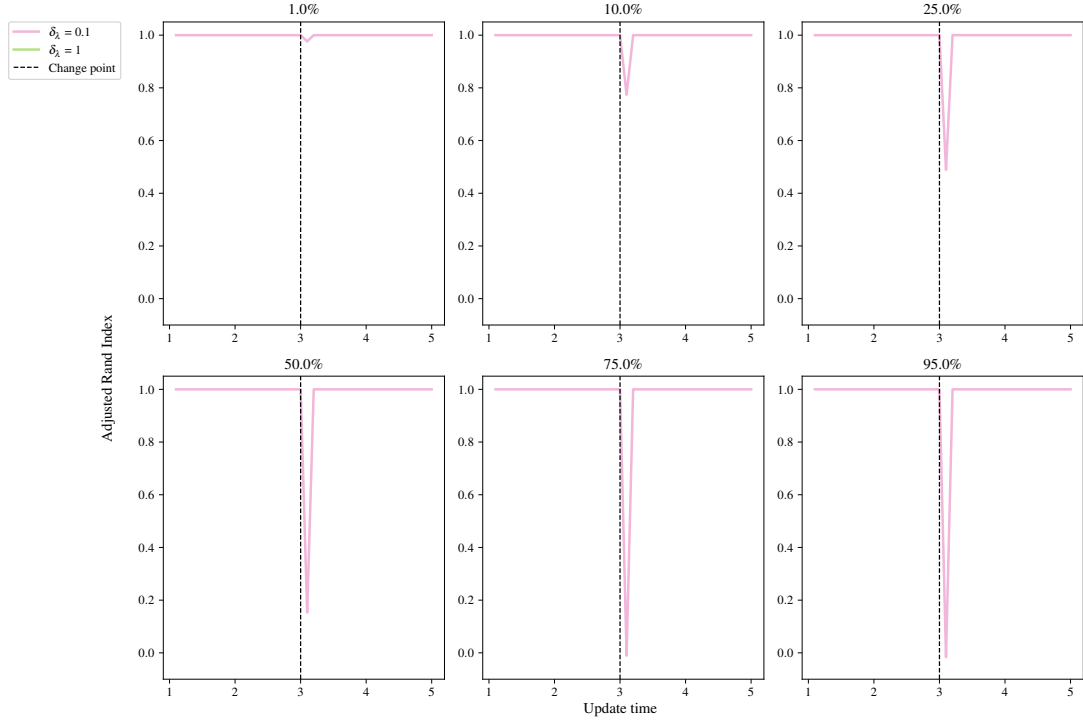
On a fully connected network, we examine sequential changes to the rate matrix with decreasing time between the changes. The rate matrix maps as

$$\lambda = \begin{pmatrix} 2 & 1 \\ 0.3 & 8 \end{pmatrix} \mapsto \lambda' = \begin{pmatrix} 5 & 1 \\ 0.3 & 8 \end{pmatrix} \mapsto \lambda'' = \begin{pmatrix} 3 & 1 \\ 0.3 & 8 \end{pmatrix},$$

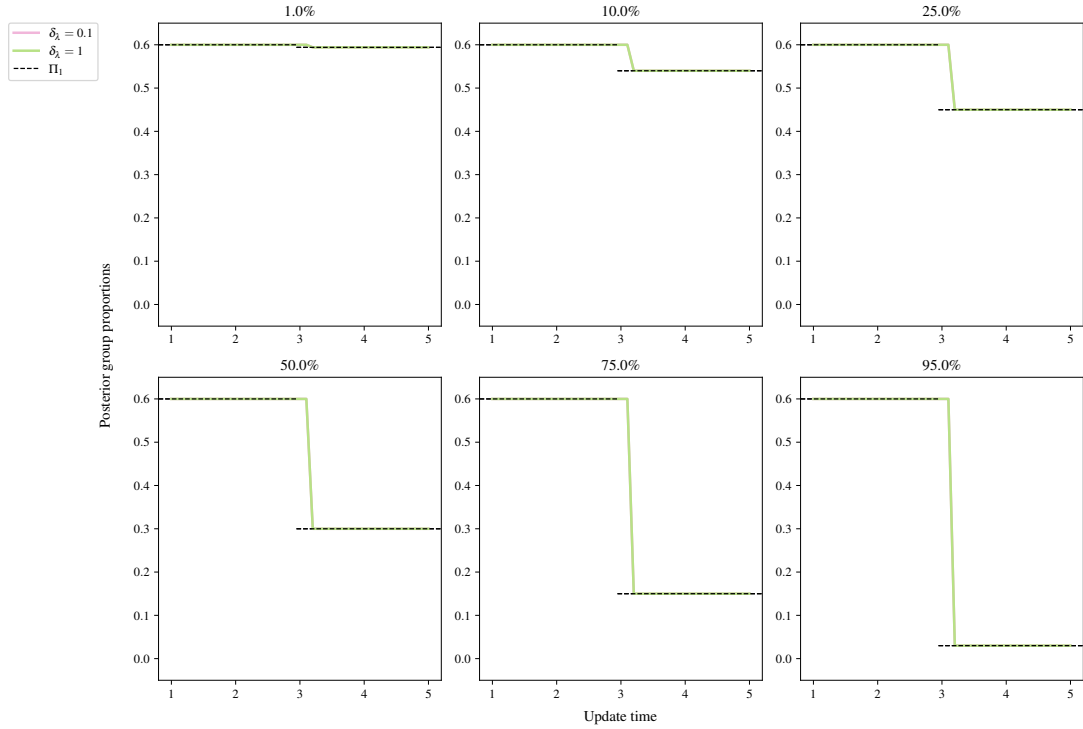
with the first change at $t = 3$ and the second at $t = 3 + 0.1M$. For each run, M took a value in $\{1, 2, 3, 4, 5, 10\}$. Here we do not reset the stream after a flagged change to the latent rates as we control their relative magnitude and wish to examine the performance of the algorithm with small latency between changes.

We evaluate the detection of latent changes using the proportion of changepoints correctly detected (CCD), and the proportion of detections that are not false (DNF), as in [Bodenham and Adams \(2017\)](#). Note that we aggregate across all group-to-group rates. Specifically, if there are C changepoints, and we detect D , T of which are correct, analogous to recall and precision, the authors define:

1. $\text{CCD} = T/C$, the proportion of changepoints correctly detected,
2. $\text{DNF} = T/D$, the proportion of detections that are not false.



(a) Mean ARI of the repetitions against update time for a varying proportion of group 1 nodes changing to group 2.



(b) Mean over the repetitions of the proportion of nodes in group 1 with time. The results obtained when using no BFF (green line) and a BFF of 0.1 (pink line) are shown together on each panel. The true proportion of group 1 either side of the changepoint is plotted as black, horizontal lines..

Figure 9: Detection of group membership changes for a varying percentage of nodes swapping from group 1 to group 2 at $t = 3$. The panel titles give the percentage of nodes that swap from group 1 to 2.

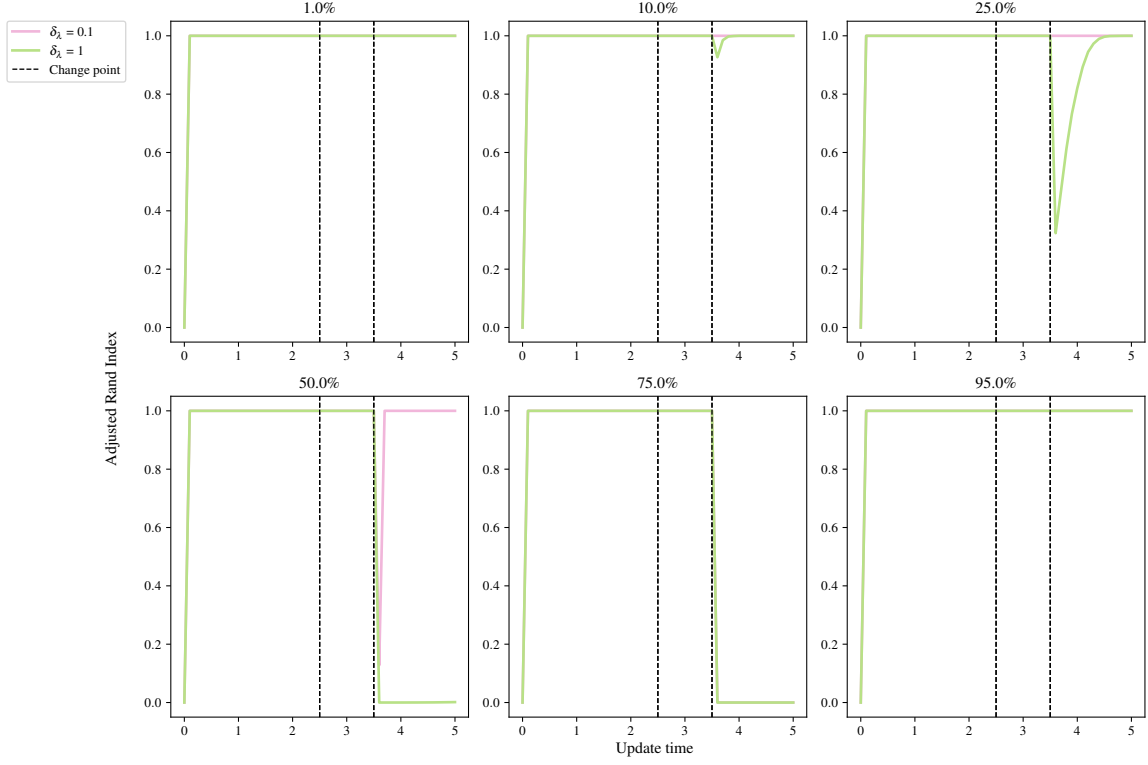


Figure 10: Mean ARI against update time for the merger of group 2 into 1 at $t = 2.5$, and the creation of group 2 at $t = 3.5$, with the panel titles giving the percentage of nodes remaining in group 1 after $t = 3.5$. The black, dashed vertical lines mark the changepoints. At $t = 2.5$, all nodes in group 2 change to group 1, and at $t = 3.5$, $P\%$ of group 1 nodes change to group 2, $P \in \{1, 10, 25, 50, 75, 95\}$.

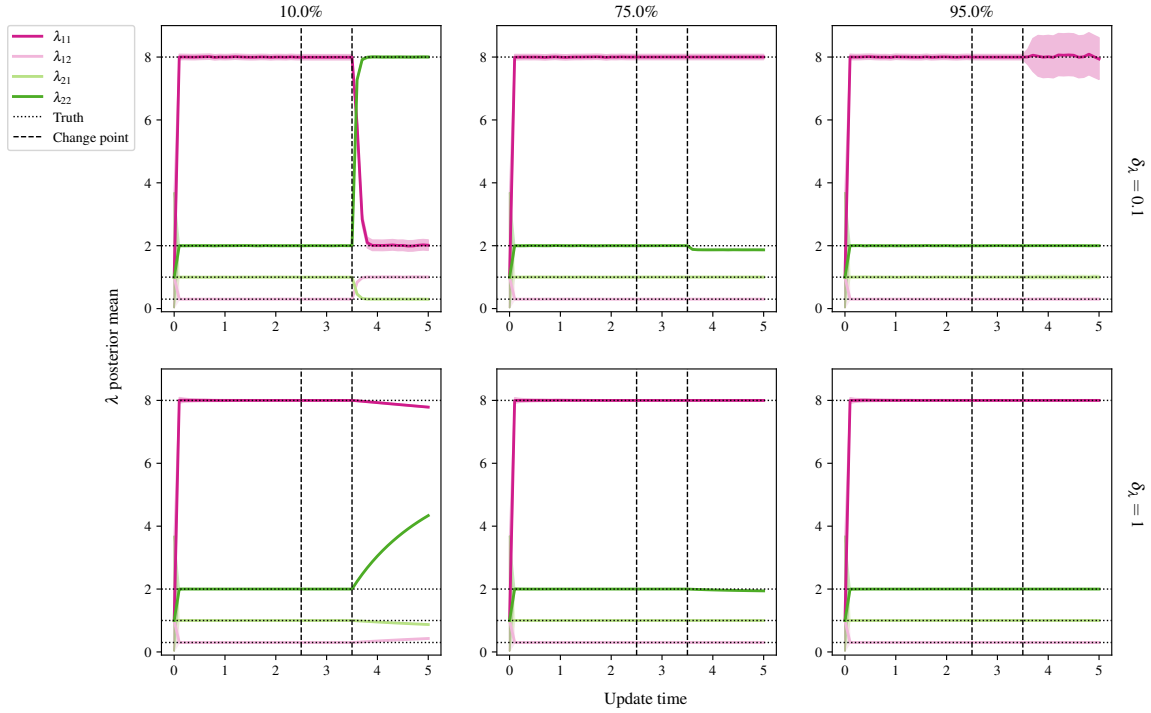


Figure 11: Posterior means and 95% simulation interval for components λ with update time. The black, dashed vertical lines mark the changepoints. At $t = 2.5$, all nodes in group 2 change to group 1, and at $t = 3.5$, $P\%$ of group 1 nodes change to group 2, $P \in \{10, 75, 95\}$.

As noted by Bodenham and Adams (2017), CCD and DNF are preferred to their more intuitive counterparts (proportion of missed changepoints and proportion of false detections, respectively) as for the CCD and DNF, values closer to 1 indicate better performance than those closer to 0. Furthermore, these metrics are preferable over the popular average run length metrics (ARL0 and ARL1; ?) as we want to capture the number of changes detected and missed.

Suppose t_n^* and t_{n+1}^* are consecutive true changepoints for λ_{km} , and let the most recently flagged changepoint by the algorithm for λ_{km} be $t'_\ell < t_n^*$. If the next flag for λ_{km} occurs at $t'_{\ell+1} > t_{n+1}^*$, that is t_n^* is missed, then t'_{m+1} is classified as a correct detection of t_{n+1}^* . This is common practice in the literature. This approach is adopted by Bodenham and Adams (2017), whereas other authors implement a softmax rule for classification (see, for example, Alanqary et al., 2021; Yamanishi and Takeuchi, 2002; Bodenham and Adams, 2017), adjusting for when multiple changes are flagged in the same window.

In Figure 12, we see the CCD and DNF for each run. The CCD is consistently high for both a BFF and no BFF. This demonstrates that the algorithm consistently flags true changes with and without a BFF. The role of the BFF is shown in the DNF, where we see BFF yielding higher values. Without a BFF, multiple changes are flagged that did not occur.

4.4 Effect of network sparsity

We examine the effect of decreasing network sparsity on changepoint detection. We simulate a network with $K' = 1$ latent connection groups, letting ρ , the group connection probability, vary over $\{0.01, 0.025, 0.05, 0.1, 0.25, 0.5\}$. For the point process groups, we retain the same Π as before, and again, we set $\lambda = \lambda_0$. We simulate on $[0, 25]$, with $\Delta = 0.1$, and at $t = 10$, 25% of nodes from group 1 swap to group 2. The inference procedure is run on the simulated network twice, once where the network is assumed fully-connected, and a second time using the SBM-BHPP. Both procedures are run with $\delta = 0.1$.

Figure 14 demonstrates the effect of incorrectly assuming that the graph is fully connected: the rates are significantly underestimated. On the other hand, when \mathbf{A} is inferred, the posterior means are much closer to the true values, even in the case of 1% density. Furthermore, in Figure 15 the mean ARI of the membership recovery is seen to be higher for the inferred adjacency matrix.

4.5 Detection of group changes with varying rates

On a fully connected network, we examine the recovery of group memberships with $K = 3$ when the latent rates also vary. We simulate a network where the latent rates vary as follows:

$$\lambda(t) = \begin{pmatrix} 2s(t) + 5 & 0.1s(t) + 0.2 & 0.05s(t) + 0.1 \\ 0.2c(t) + 1 & c(t) + 2 & 0.01s(t) + 0.8 \\ 0.1c(t) + 0.9 & 0.1s(t) + 0.5 & 0.01c(t) + 0.03 \end{pmatrix},$$

where $s(t) = \sin(2\pi t/5)$ and $c(t) = \cos(2\pi t/5)$. In the simulation, we set $\Pi = (0.4, 0.4, 0.2)$ and at $t = 3.05$, 25% of the nodes change from group 1 to either group 2 or 3. We use a BFF of 0.1 with the standard BHPP model. Figure 16 shows the posterior means of the rates and the ARI with update. We see that the rates are well-recovered and the ARI remains high either side of the change.

5 Application to the Santander Cycles bike-sharing network

The proposed online changepoint algorithms were tested on Transport for London (TfL) data from the London Santander Cycles bike-sharing network, which is publicly available online (<https://cycling.data.tfl.gov.uk/>, powered by TfL Open Data). Each datum corresponds to a bike hire, and contains the start and end times of the journey, the IDs of the source and destination stations, the journey duration, a bike ID number, and an unique identifier for the journey. Considering the start and end stations as source and destination nodes, and the timestamp of the end of the journey as an arrival time to the directed edge from source to destination, the data forms a network point process. In this study, the data is aggregated into weekly counts to smooth the intensities

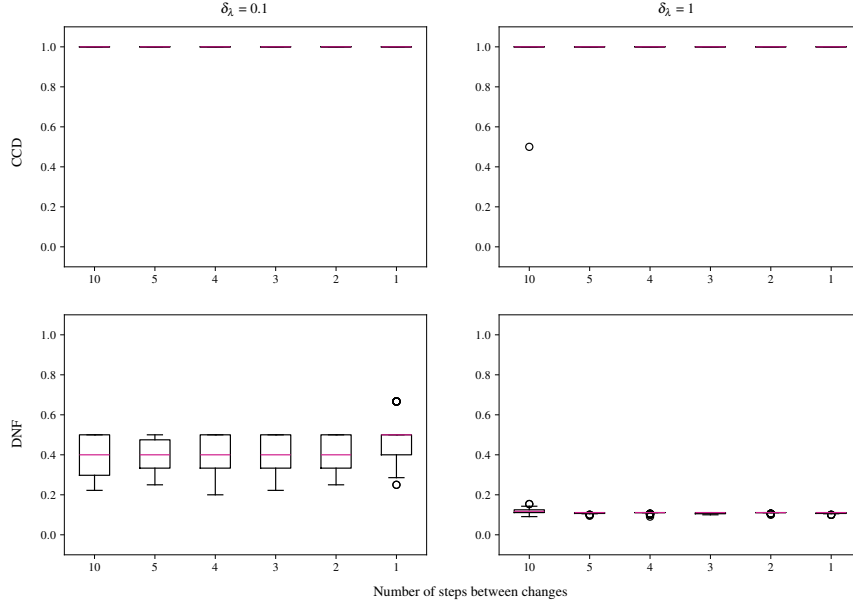


Figure 12: Boxplots of CCD and DNF over 50 runs for no BFF and a BFF of $\delta = 0.1$. Each simulation has one change at $t = 3$ and another at $t = 3 + 0.1M$, where M is on the horizontal axis.

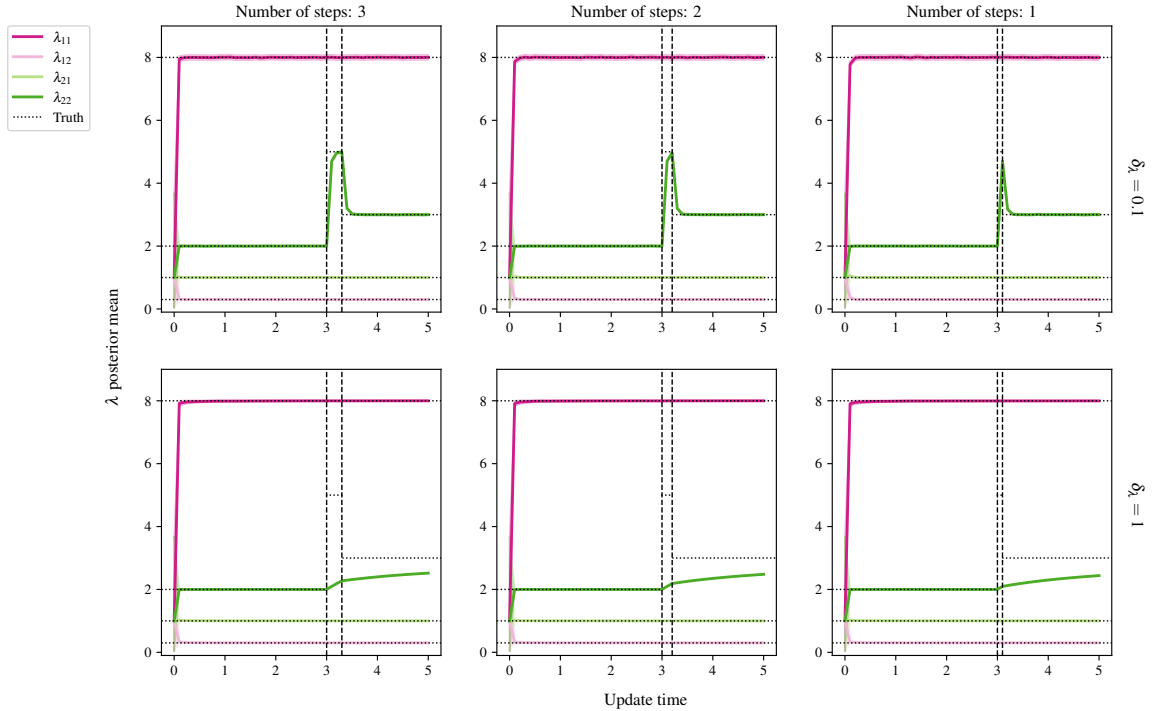


Figure 13: Posterior means and 95% simulation interval for components λ with update time. The black, dashed vertical lines mark the changepoints. Each simulation has one change at $t = 3$ and another at $t = 3 + 0.1M$, where M is the number of time steps in the column caption.

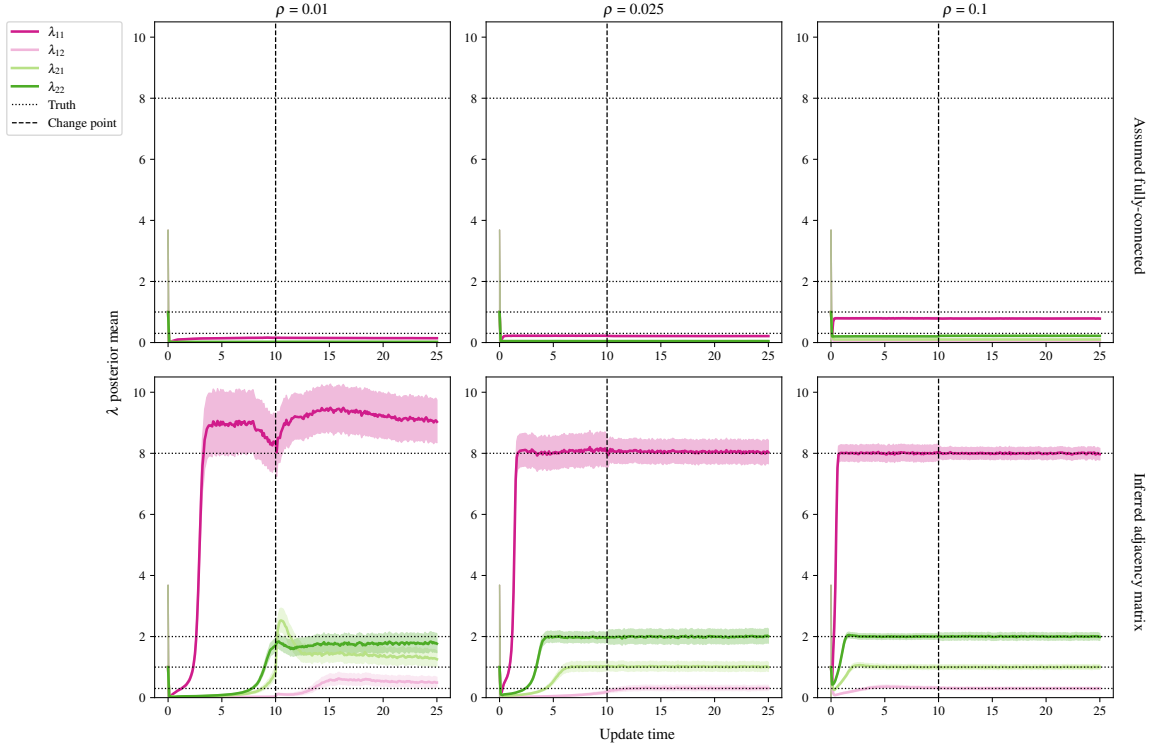


Figure 14: Posterior means and 95% simulation interval for components λ with update time. The black, dashed vertical line marks the changepoint, at which 25% of nodes in group 1 swap to group 2.

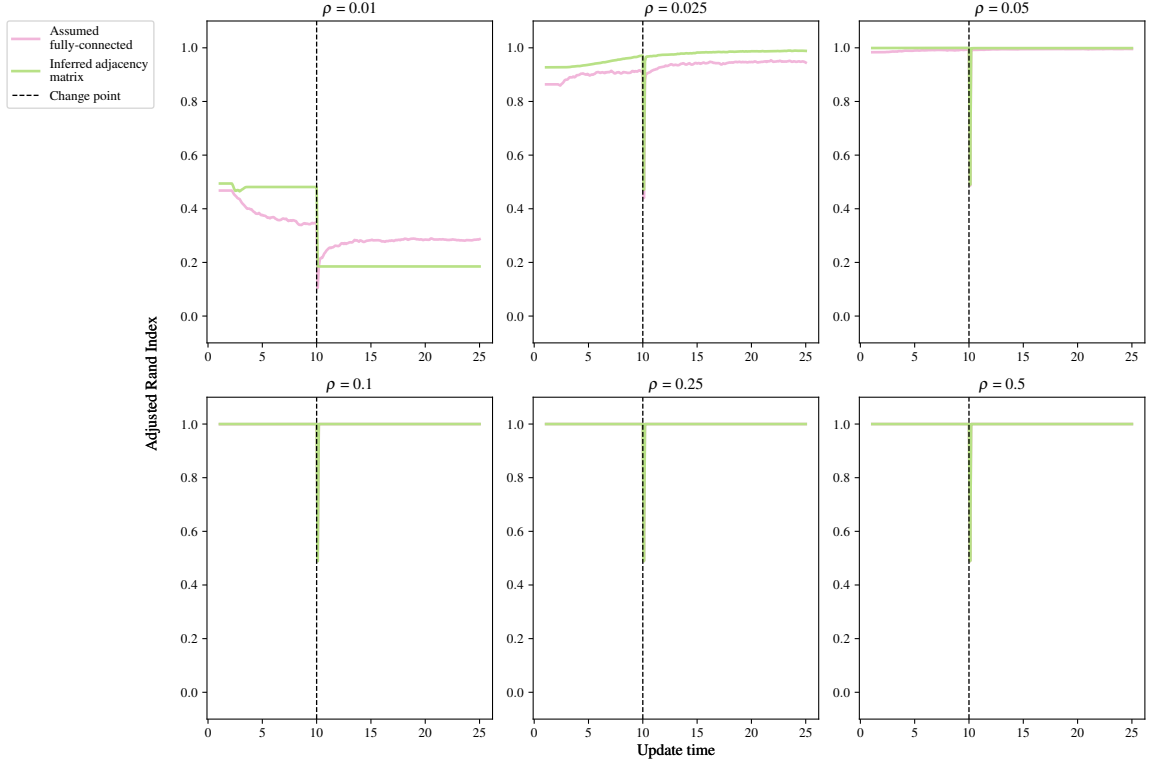


Figure 15: Mean ARI of the repetitions against update time. The black, dashed vertical line marks the changepoint, at which 25% of nodes in group 1 swap to group 2.

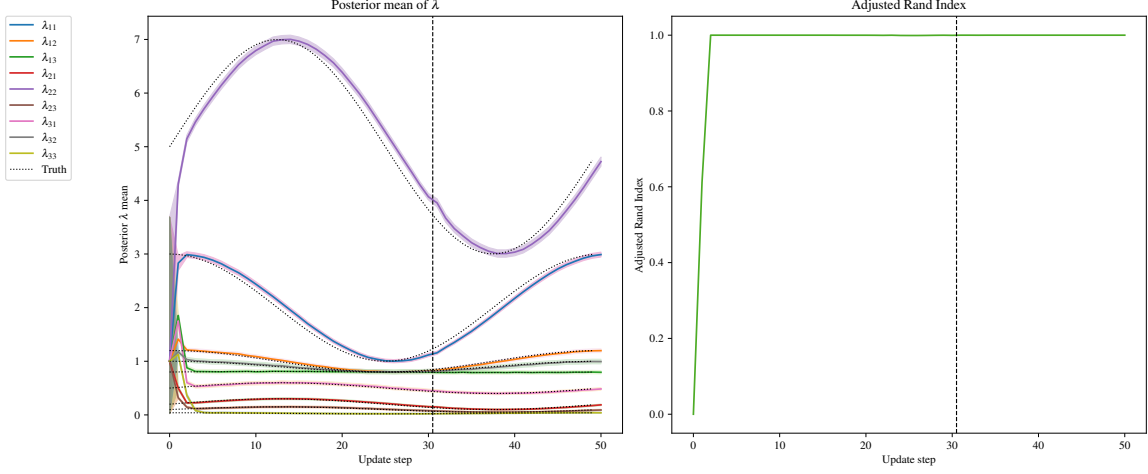


Figure 16: Left-panel: posterior means and 95% simulation interval for the components λ with update time. The black, dotted lines are the true underlying rates. Right-panel: ARI with update time. The black, dashed vertical line marks the changepoint.

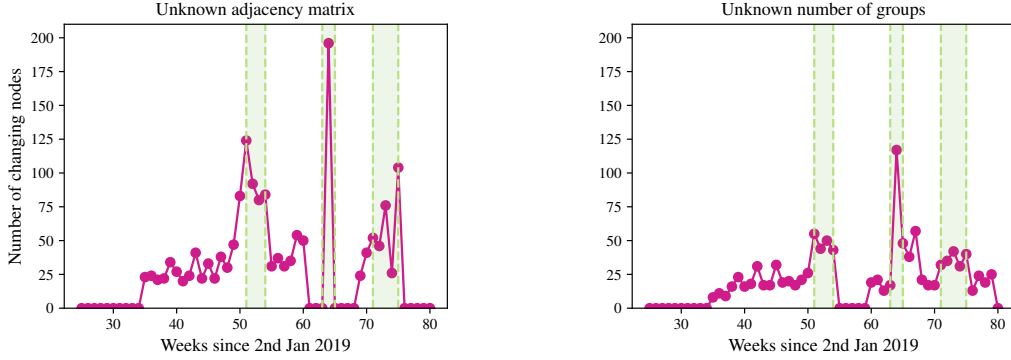


Figure 17: The number of nodes that change memberships at each update point from initialisation. The green regions correspond to the Christmas and New Year period of 2019, the introduction of the first UK COVID-19 lockdown, and the phased easing of these restrictions, respectively.

of the point processes and weekly periodicities. Despite the smoothing, we do not satisfy the homogeneous Poisson assumption, and thus look to infer changes to the latent groups and not to the latent rates. In Section 4.5, we demonstrate through simulation that we are able to do this. We select a subset of the data from 2nd January 2019 until 15th July 2020 as this window contains significant COVID-19 related national events that can be used to check the performance of our algorithm. In this time period, $N = 791$ unique nodes are observed within $T = 80$ weekly time windows, with updates every $\Delta = 1$ week time steps.

The online VB algorithm for the dynamic BHPP is run for the separate cases of the SBM-BHPP and the GEM-BHPP. The number of groups in the case of an unknown adjacency matrix was set to match the number inferred by the implementation for an unknown number of groups, which was $K = 6$. The adjacency matrix in the case of unknown K was set to correspond to a fully connected graph: $\mathbf{A} = \mathbf{1}_{791 \times 791}$. We consider the task of detecting changes to the latent group structure of the bike sharing network. We run both algorithms with $W_{JS} = 1.55$, $B_1 = 25$, $B_2 = 10$, and $\kappa = 2$, so that changes can be detected only after $B_1 + B_2 + \kappa = 37$ weeks of observations. We initialise the hyperparameters as described in Section 4.

Figure 17 shows that both algorithms flag multiple changes at each update, but that there are three regions where the number of flagged changes peaks. From left to right, these green regions correspond to the Christmas and New Year period of 2019, the introduction of the first UK COVID-19 lockdown on 19/03/2020, and the subsequent phased easing of restrictions from 01/06/2020. The algorithm reacts to these events, which are likely to cause changes to the network.

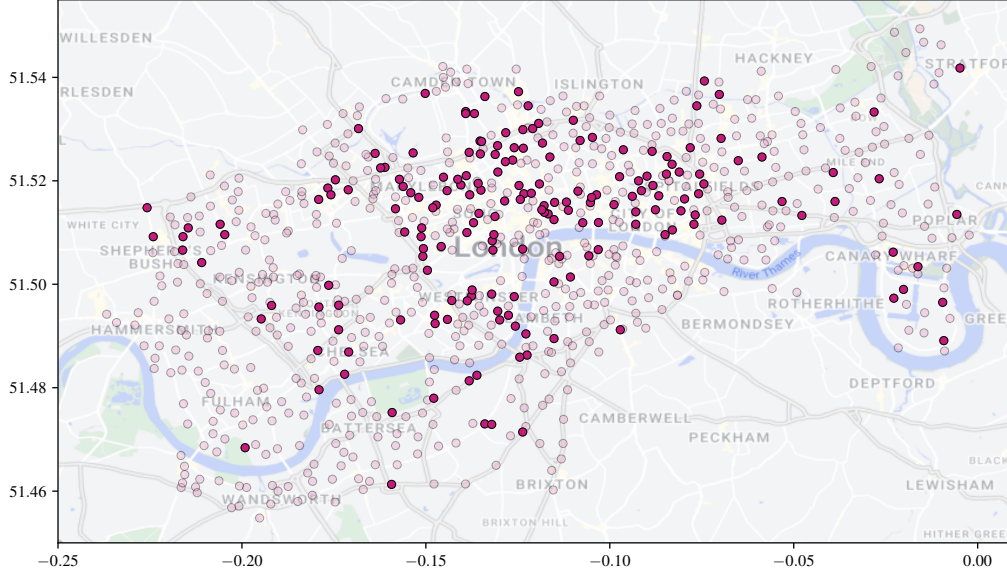


Figure 18: Station locations with those stations that change group at the onset of the UK COVID-19 lockdown coloured dark red.

Figure 18 shows that the flagged changes from the SBM-BHPP corresponding to the onset of the lockdown are very concentrated around central London, which makes sense as “work from home” orders will have affected the use of these commuting bike stations. Additionally, stations around the Westfield Shopping Centre in Shepherd’s Bush and the Canary Wharf financial district are flagged, representing an expected change due to the government restrictions.

Furthermore, Figure 19 displays an example clustering from the GEM-BHPP at update point 50. There is some spatial clustering to the nodes, but each cluster contains mainly nodes with similar activity patterns. For example, the dark and light blue clusters represent popular nodes in central London and the Canary Wharf financial district, which are mainly used by commuters into these areas. Similarly, the light and dark green clusters are nodes in West and East London (with the dark green cluster mostly covering West London, and the light green East London and the areas of Battersea and Wandsworth (south of the river Thames). The pink cluster is around the boundary between the blue and green regions. A notable exception is represented by the red cluster, representing the most popular stations within the network, mainly used for leisure around Hyde Park and the Queen Elizabeth Olympic Park in Stratford. In addition, the red cluster also contains two additional stations in Battersea Park and Ravenscourt Park (west of Hammersmith).

6 Conclusion and discussion

We have presented a novel online Bayesian inference framework for detecting changes to the latent structure of a block-homogeneous Poisson process in which data arrives as batches in an event stream. Our methodology is scalable, and leverages a Bayesian forgetting factor framework to flag changes to the latent community structure and edge-process rates. The framework is extended to the cases where the adjacency matrix or the number of latent groups are unknown a priori. When tested on both real and simulated data, our methodology is seen to detect latent structure accurately and with minimal latency.

There are numerous ways in which this work could be extended. In particular, the frameworks for an unknown graph structure and unknown number of latent groups can readily be integrated to handle the case where neither is known a priori. It would also be of interest to incorporate seasonality into the model, perhaps within an online framework with longer memory.

A further challenge would be to adapt the framework to allow for nodes to enter or leave the network during observation. Similarly, the adjacency matrix is assumed static in our methodology, and so an extension would

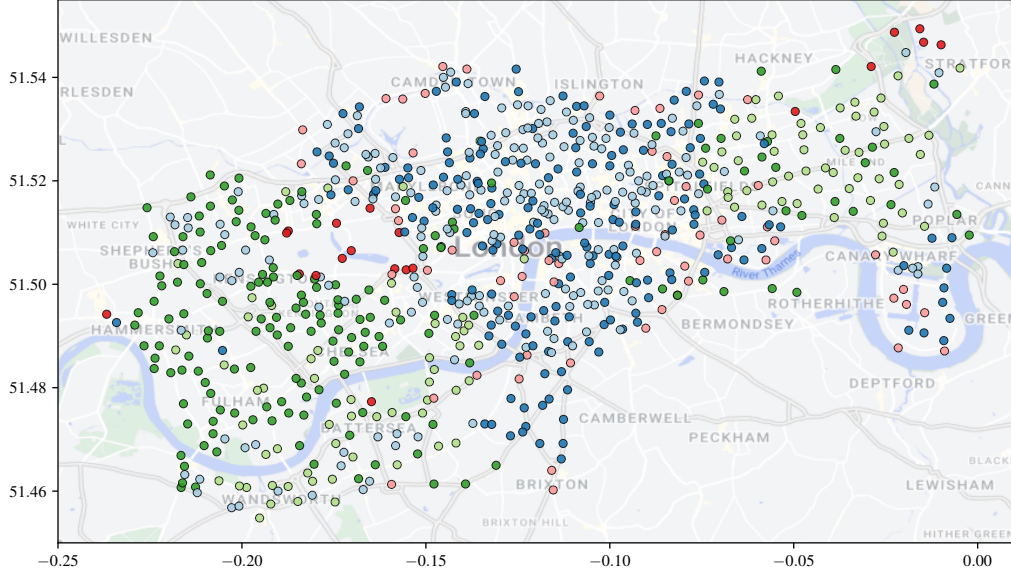


Figure 19: Station locations coloured by assigned group at update time step 50 of the dynamic BHPP with an unknown number of groups and $\mathbf{A} = \mathbf{1}_{791 \times 791}$.

allow for this to be dynamic, although this would likely cause identifiability issues in the case where there are also changes to the latent rates.

Acknowledgements

We would like to thank Professor Nick Heard and Professor Alessandra Luati for their valuable feedback on this manuscript. Joshua Corneek acknowledges funding from the Engineering and Physical Sciences Research Council (EPSRC), grant number EP/S023151/1. Ed Cohen acknowledges funding from the EPSRC NeST Programme, grant number EP/X002195/1. Francesco Sanna Passino acknowledges funding from the EPSRC, grant number EP/Y002113/1.

Code

Python code to implement the methodologies proposed in this article and reproduce the results is available in the Github repository [joshcorneek/dynamicBHPP](https://github.com/joshcorneek/dynamicBHPP).

References

- Airoldi, E. M., Costa, T. B., and Chan, S. H. (2013) Stochastic blockmodel approximation of a graphon: Theory and consistent estimation. In *Advances in Neural Information Processing Systems* (eds. C. Burges, L. Bottou, M. Welling, Z. Ghahramani and K. Weinberger), vol. 26. Curran Associates, Inc.
- Alanqary, A., Alomar, A. O., and Shah, D. (2021) Change point detection via multivariate singular spectrum analysis. In *Advances in Neural Information Processing Systems* (eds. A. Beygelzimer, Y. Dauphin, P. Liang and J. W. Vaughan).
- Amini, A. A., Chen, A., Bickel, P. J., and Levina, E. (2013) Pseudo-likelihood methods for community detection in large sparse networks. *The Annals of Statistics*, **41**, 2097–2122.
- Bifet, A., Gavaldà, R., Holmes, G., and Pfahringer, B. (2018) *Machine Learning for Data Streams: with Practical Examples in MOA*. Adaptive Computation and Machine Learning series. MIT Press.

- Bishop, C. M. (2006) *Pattern Recognition and Machine Learning (Information Science and Statistics)*. Berlin, Heidelberg: Springer-Verlag.
- Blei, D. M. and Jordan, M. I. (2006) Variational inference for Dirichlet process mixtures. *Bayesian Analysis*, **1**, 121–143.
- Blei, D. M., Kucukelbir, A., and McAuliffe, J. D. (2017) Variational inference: A review for statisticians. *Journal of the American Statistical Association*, **112**, 859–877.
- Bodenham, D. A. and Adams, N. M. (2017) Continuous monitoring for changepoints in data streams using adaptive estimation. *Statistics and Computing*, **27**, 1257–1270.
- Fang, G., Ward, O. G., and Zheng, T. (2024) Online estimation and community detection of network point processes for event streams. *Statistics and Computing*, **34**.
- Ferguson, T. S. (1973) A Bayesian analysis of some nonparametric problems. *The Annals of Statistics*, **1**, 209–230.
- Gao, C., Ma, Z., Zhang, A. Y., and Zhou, H. H. (2018) Community detection in degree-corrected block models. *The Annals of Statistics*, **46**, 2153–2185.
- Hallgren, K. L., Heard, N. A., and Turcotte, M. J. M. (2023) Changepoint detection on a graph of time series. *Bayesian Analysis*, 1–28.
- Haykin, S. (2002) *Adaptive filter theory*. Upper Saddle River, NJ: Prentice Hall, 4th edn.
- Heard, N. A., Weston, D. J., Platanioti, K., and Hand, D. J. (2010) Bayesian anomaly detection methods for social networks. *The Annals of Applied Statistics*, **4**, 645–662.
- Holland, P. W., Laskey, K. B., and Leinhardt, S. (1983) Stochastic blockmodels: First steps. *Social Networks*, **5**, 109–137.
- Holme, P. (2015) Modern temporal network theory: a colloquium. *The European Physical Journal B*, **88**, 234.
- Hubert, L. J. and Arabie, P. (1985) Comparing partitions. *Journal of Classification*, **2**, 193–218.
- Jasra, A., Holmes, C. C., and Stephens, D. A. (2005) Markov Chain Monte Carlo methods and the label switching problem in Bayesian mixture modeling. *Statistical Science*, **20**, 50–67.
- Karrer, B. and Newman, M. E. J. (2011) Stochastic blockmodels and community structure in networks. *Physical Review E*, **83**, 016107.
- Klimt, B. and Yang, Y. (2004) The Enron corpus: A new dataset for email classification research. In *Machine Learning: ECML 2004* (eds. J.-F. Boulicaut, F. Esposito, F. Giannotti and D. Pedreschi), 217–226. Berlin, Heidelberg: Springer Berlin Heidelberg.
- Lee, C. and Wilkinson, D. J. (2019) A review of stochastic block models and extensions for graph clustering. *Applied Network Science*, **4**, 1–50.
- Leys, C., Ley, C., Klein, O., Bernard, P., and Licata, L. (2013) Detecting outliers: Do not use standard deviation around the mean, use absolute deviation around the median. *Journal of Experimental Social Psychology*, **49**, 764–766.
- Lin, J. (1991) Divergence measures based on the Shannon entropy. *IEEE Transactions on Information Theory*, **37**, 145–151.
- Mariadassou, M., Robin, S., and Vacher, C. (2010) Uncovering latent structure in valued graphs: A variational approach. *The Annals of Applied Statistics*, **4**.

- Mariadassou, M. and Tabouy, T. (2020) Consistency and asymptotic normality of stochastic block models estimators from sampled data. *The Electronic Journal of Statistics*, **14**, 3672–3704.
- Matias, C. and Miele, V. (2017) Statistical clustering of temporal networks through a dynamic stochastic block model. *Journal of the Royal Statistical Society. Series B (Statistical Methodology)*, **79**, 1119–1141.
- Matias, C., Rebafka, T., and Villers, F. (2018) A semiparametric extension of the stochastic block model for longitudinal networks. *Biometrika*, **105**, 665–680.
- Paranjape, A., Benson, A. R., and Leskovec, J. (2017) Motifs in temporal networks. In *Proceedings of the Tenth ACM International Conference on Web Search and Data Mining, WSDM '17*, 601–610. New York, NY, USA: Association for Computing Machinery.
- Perry, P. O. and Wolfe, P. J. (2013) Point process modelling for directed interaction networks. *Journal of the Royal Statistical Society Series B: Statistical Methodology*, **75**, 821–849.
- Pitman, J. (2002) Combinatorial stochastic processes (Technical Report 621). Department of Statistics. *University of California at Berkeley, Berkeley, CA*.
- Ray, K. and Szabó, B. (2022) Variational Bayes for high-dimensional linear regression with sparse priors. *Journal of the American Statistical Association*, **117**, 1270–1281.
- Sanna Passino, F. and Heard, N. A. (2023) Mutually exciting point process graphs for modeling dynamic networks. *Journal of Computational and Graphical Statistics*, **32**, 116–130.
- Sethuraman, J. (1994) A constructive definition of Dirichlet priors. *Statistica Sinica*, 639–650.
- Shlomovich, L., Cohen, E. A. K., and Adams, N. (2022) A parameter estimation method for multivariate binned Hawkes processes. *Statistics and Computing*, **32**, 98.
- van Dyk, D. A. and Park, T. (2008) Partially collapsed Gibbs samplers. *Journal of the American Statistical Association*, **103**, 790–796.
- Wang, Y. and Blei, D. M. (2019) Frequentist consistency of variational Bayes. *Journal of the American Statistical Association*, **114**, 1147–1161.
- Xu, K. and Hero, A. (2014) Dynamic stochastic blockmodels for time-evolving social networks. *IEEE Journal of Selected Topics in Signal Processing*, **8**, 552–562.
- Yamanishi, K. and Takeuchi, J. (2002) A unifying framework for detecting outliers and change points from non-stationary time series data. In *Proceedings of the Eighth ACM SIGKDD International Conference on Knowledge Discovery and Data Mining, KDD '02*, 676–681. New York, NY, USA: Association for Computing Machinery.
- Yang, T., Chi, Y., Zhu, S., Gong, Y., and Jin, R. (2011) Detecting communities and their evolutions in dynamic social networks - a Bayesian approach. *Machine Learning*, **82**, 157–189.
- Zhang, A. Y. and Zhou, H. H. (2020) Theoretical and computational guarantees of mean field variational inference for community detection. *The Annals of Statistics*, **48**, 2575–2598.

Appendix A Derivation of CAVI updates

Here we derive the CAVI approximating distributions for each parameter at the r th update. In deriving these expressions, we assume no ordering for the parameter updates, and will use a superscript of $(r - 1)$ for all parameters but for the one whose expression is then being derived.

A.1 Approximation of $q(z_i)$

Ignoring any terms that do not contain z_i , we can derive the expectation as follows:

$$\begin{aligned}
 \mathbb{E}_{-z_i} \{\log p(x, z, \lambda, \pi)\} &= \mathbb{E}_{-z_i} \{\log p(x|z, \lambda) + \delta_z \log p(z|\pi)\} + \text{cst.} \\
 &= \mathbb{E}_{-z_i} \left[\sum_{j:(i,j) \in \mathcal{E}} \sum_{k,m \in \mathcal{K}} \tilde{z}_{ik} \tilde{z}_{jm} \left(x_{ij}(I_r) \log(\lambda_{km}) - \Delta \lambda_{km} \right) + \right. \\
 &\quad \sum_{j':(j',i) \in \mathcal{E}} \sum_{k,m \in \mathcal{K}} \tilde{z}_{j'k} \tilde{z}_{im} \left(x_{j'i}(I_r) \log(\lambda_{km}) - \Delta \lambda_{km} \right) - \\
 &\quad \left. \sum_{k \in \mathcal{K}} \tilde{z}_{ik} \left(x_{ii}(t) \log(\lambda_{kk}) - \Delta \lambda_{kk} \right) + \delta_z \sum_{k \in \mathcal{K}} \tilde{z}_{ik} \log \pi_k \right] + \text{cst.} \\
 &= \sum_{k \in \mathcal{K}} \tilde{z}_{ik} \left[\delta_z \mathbb{E}_\pi \{\log \pi_k\} + x_{ii}(t) \mathbb{E}_{\lambda_{kk}} \{\log(\lambda_{kk})\} - \Delta \mathbb{E}_{\lambda_{kk}} \{\lambda_{kk}\} + \right. \\
 &\quad \sum_{m \in \mathcal{K}} \left\{ \sum_{j:(i,j) \in \mathcal{E}} \mathbb{E}_{z_j} \{\tilde{z}_{jm}\} \left(x_{ij}(I_r) \mathbb{E}_{\lambda_{km}} \{\log(\lambda_{km})\} - \Delta \mathbb{E}_{\lambda_{km}} \{\lambda_{km}\} \right) \left(1 - \mathbb{I}_{\{k\}}(m) \mathbb{I}_{\{i\}}(j) \right) + \right. \\
 &\quad \left. \left. \sum_{j':(j',i) \in \mathcal{E}} \mathbb{E}_{z_{j'}} \{\tilde{z}_{j'm}\} \left(x_{j'i}(I_r) \mathbb{E}_{\lambda_{mk}} \{\log(\lambda_{mk})\} - \Delta \mathbb{E}_{\lambda_{mk}} \{\lambda_{mk}\} \right) \left(1 - \mathbb{I}_{\{k\}}(m) \mathbb{I}_{\{i\}}(j') \right) \right\} \right] + \text{cst.}
 \end{aligned}$$

Taking the exponential, it follows that the optimal choice of $\hat{q}(z_i)$ under a CAVI approximation is $\hat{q}^{(r)}(z_i) = \text{Categorical}(z_i; \tau_i^{(r)})$, where

$$\begin{aligned}
 \tau_{ik}^{(r)} &\propto \exp \left\{ \delta_z \left[\psi \left(\gamma_k^{(r-1)} \right) - \psi \left(\sum_{\ell} \gamma_{\ell}^{(r-1)} \right) \right] + x_{ii}(t) \left(\psi \left(\alpha_{kk}^{(r-1)} \right) - \log \left(\beta_{kk}^{(r-1)} \right) \right) - \Delta \frac{\alpha_{kk}^{(r-1)}}{\beta_{kk}^{(r-1)}} + \right. \\
 &\quad \sum_{m \in \mathcal{K}} \left[\sum_{j:(i,j) \in \mathcal{E}} \tau_{jm}^{(r-1)} \left(x_{ij}(I_r) \left(\psi \left(\alpha_{km}^{(r-1)} \right) - \log \left(\beta_{km}^{(r-1)} \right) \right) - \Delta \frac{\alpha_{km}^{(r-1)}}{\beta_{km}^{(r-1)}} \right) \left(1 - \mathbb{I}_{\{k\}}(m) \mathbb{I}_{\{i\}}(j) \right) + \right. \\
 &\quad \left. \left. \sum_{j':(j',i) \in \mathcal{E}} \tau_{j'm}^{(r-1)} \left(x_{j'i}(I_r) \left(\psi \left(\alpha_{mk}^{(r-1)} \right) - \log \left(\beta_{mk}^{(r-1)} \right) \right) - \Delta \frac{\alpha_{mk}^{(r-1)}}{\beta_{mk}^{(r-1)}} \right) \left(1 - \mathbb{I}_{\{k\}}(m) \mathbb{I}_{\{i\}}(j') \right) \right] \right\},
 \end{aligned}$$

for $i \in \mathcal{V}$ and $k \in \mathcal{K}$.

A.2 Approximation of $q(\pi)$

Ignoring any terms that do not contain π , we compute the expectation as:

$$\begin{aligned}
 \mathbb{E}_{-\pi} \{\log p(x, z, \lambda, \pi)\} &= \mathbb{E}_{-\pi} \{\delta_z \log p(z|\pi) + \delta_\pi \log p(\pi)\} + \text{cst.} \\
 &= \sum_{k \in \mathcal{K}} \log \pi_k \left[\sum_{i \in \mathcal{V}} \delta_z \mathbb{E}_{z_i} \{\tilde{z}_{ik}\} + \delta_\pi \left(\gamma_k^{(r-1)} - 1 \right) \right] + \text{cst.}
 \end{aligned}$$

Using the distributions derived for $\hat{q}^{(r-1)}(z_i)$, we see that the optional CAVI approximation is to take $\hat{q}^{(r)}(\pi) = \text{Dirichlet}(\pi; \gamma^{(r)})$, where

$$\gamma_k^{(r)} = \delta_\pi \left(\gamma_k^{(r-1)} - 1 \right) + \delta_z \sum_{i \in \mathcal{V}} \tau_{ik}^{(r-1)} + 1,$$

for $k \in \mathcal{K}$.

A.3 Approximation of $q(\lambda_{km})$

Ignoring any terms that do not contain λ_{km} , we derive the expectation as follows:

$$\begin{aligned} \mathbb{E}_{-\lambda_{km}} \{ \log p(x, z, \lambda, \pi) \} &= \mathbb{E}_{-\lambda_{km}} \{ \log p(x|z, \lambda) + \delta_\lambda \log p(\lambda) \} + \text{cst.} \\ &= \sum_{(i,j) \in \mathcal{E}} \sum_{k,m \in \mathcal{K}} \left[\mathbb{E}_{z_i} \{ \tilde{z}_{ik} \} \mathbb{E}_{z_j} \{ \tilde{z}_{jm} \} (x_{ij} \log \lambda_{km} - \lambda_{km} \Delta) \right] + \\ &\quad \delta_\lambda \sum_{k,m \in \mathcal{K}} \left[\left(\alpha_{km}^{(r-1)} - 1 \right) \log \lambda_{km} - \beta_{km}^{(r-1)} \lambda_{km} \right] + \text{cst.} \\ &= \sum_{k,m \in \mathcal{K}} \left\{ \left(\delta_\lambda \left(\alpha_{km}^{(r-1)} - 1 \right) + \sum_{(i,j) \in \mathcal{E}} \mathbb{E}_{z_i} \{ \tilde{z}_{ik} \} \mathbb{E}_{z_j} \{ \tilde{z}_{jm} \} x_{ij} (I_r) \right) \log \lambda_{km} - \right. \\ &\quad \left. \left(\delta_\lambda \beta_{km}^{(r-1)} + \Delta \sum_{(i,j) \in \mathcal{E}} \mathbb{E}_{z_i} \{ \tilde{z}_{ik} \} \mathbb{E}_{z_j} \{ \tilde{z}_{jm} \} \right) \lambda_{km} \right\} + \text{cst.} \end{aligned}$$

Using the distributions derived for $\hat{q}^{(r-1)}(z_i)$, it follows that the optimal CAVI approximation is to take $\hat{q}^{(r)}(\lambda_{km}) = \text{Gamma}(\lambda_{km}; \alpha_{km}^{(r)}, \beta_{km}^{(r)})$, where

$$\begin{aligned} \alpha_{km}^{(r)} &= \delta_\lambda \left(\alpha_{km}^{(r-1)} - 1 \right) + \sum_{(i,j) \in \mathcal{E}} \tau_{ik}^{(r-1)} \tau_{jm}^{(r-1)} x_{ij} (I_r) + 1, \\ \beta_{km}^{(r)} &= \delta_\lambda \beta_{km}^{(r-1)} + \Delta \sum_{(i,j) \in \mathcal{E}} \tau_{ik}^{(r-1)} \tau_{jm}^{(r-1)}, \end{aligned}$$

for $k, m \in \mathcal{K}$.

Appendix B Derivation of CAVI updates for an unknown adjacency matrix

Here we derive the CAVI approximating distributions for each parameter at the r th update. In deriving these expressions, we assume no ordering for the parameter updates, and will use a superscript of $(r-1)$ for all parameters but for the one whose expression is then being derived.

B.1 Approximation of $q(z_i)$

Ignoring any terms that do not contain z_i , we derive the expectation as:

$$\begin{aligned} \mathbb{E}_{-z_i} \{ \log p(x, z, a, \lambda, \pi) \} &= \mathbb{E}_{-z_i} \{ \log p(x|z, a, \lambda) + \delta_z \log p(z|\pi) \} + \text{cst.} \\ &= \mathbb{E}_{-z_i} \left\{ \sum_{j \in \mathcal{V}} \sum_{k,m \in \mathcal{K}} \tilde{z}_{ik} \tilde{z}_{jm} \left[a_{ij} (x_{ij} (I_r) \log \lambda_{km} - \Delta \lambda_{km}) \right] + \right. \\ &\quad \sum_{j' \in \mathcal{V}} \sum_{k,m \in \mathcal{K}} \tilde{z}_{j'k} \tilde{z}_{im} \left[a_{j'i} (x_{j'i} (I_r) \log \lambda_{km} - \Delta \lambda_{km}) \right] - \\ &\quad \left. \sum_{k \in \mathcal{K}} \tilde{z}_{ik} \left[a_{ii} (x_{ii} (I_r) \log \lambda_{kk} - \Delta \lambda_{kk}) \right] + \delta_z \sum_{k \in \mathcal{K}} \tilde{z}_{ik} \log \pi_k \right\} + \text{cst.} \end{aligned}$$

$$\begin{aligned}
 &= \mathbb{E}_{-z_i} \left\{ \sum_{j \in \mathcal{V}} \sum_{k, m \in \mathcal{K}} \tilde{z}_{ik} \tilde{z}_{jm} \left[a_{ij} (x_{ij}(I_r) \log \lambda_{km} - \Delta \lambda_{km}) + a_{ji} (x_{ji}(I_r) \log \lambda_{mk} - \Delta \lambda_{mk}) \right] - \right. \\
 &\quad \left. \sum_{k \in \mathcal{K}} \tilde{z}_{ik} \left[a_{ii} (x_{ii}(I_r) \log \lambda_{kk} - \Delta \lambda_{kk}) \right] + \delta_z \sum_{k \in \mathcal{K}} \tilde{z}_{ik} \log \pi_k \right\} + \text{cst.} \\
 &= \sum_{k \in \mathcal{K}} \tilde{z}_{ik} \left\{ \sum_{j \in \mathcal{V}} \sum_{m \in \mathcal{K}} \tilde{z}_{jm} \left[x_{ij}(I_r) \mathbb{E}_{a_{ij}} \{a_{ij}\} \mathbb{E}_{\lambda_{km}} \{\log \lambda_{km}\} + x_{ji}(I_r) \mathbb{E}_{a_{ji}} \{a_{ji}\} \mathbb{E}_{\lambda_{mk}} \{\log \lambda_{mk}\} - \right. \right. \\
 &\quad \left. \left. \Delta \left(\mathbb{E}_{a_{ij}} \{a_{ij}\} \mathbb{E}_{\lambda_{km}} \{\lambda_{km}\} + \mathbb{E}_{a_{ji}} \{a_{ji}\} \mathbb{E}_{\lambda_{mk}} \{\lambda_{mk}\} \right) \right] \left(1 - \mathbb{I}_{\{k\}}(m) \mathbb{I}_{\{i\}}(j) \right) + \right. \\
 &\quad \left. \mathbb{E}_{a_{ii}} \{a_{ii}\} \left(x_{ii}(I_r) \mathbb{E}_{\lambda_{kk}} \{\log \lambda_{kk}\} - \Delta \mathbb{E}_{\lambda_{kk}} \{\lambda_{kk}\} \right) + \delta_z \mathbb{E}_{\pi_k} \{\log \pi_k\} \right\} + \text{cst.}
 \end{aligned}$$

Taking the exponential, and using the distributions derived for $\hat{q}^{(r-1)}(\lambda_{km})$ and the assumed form for $\hat{q}^{(r-1)}(a_{ij})$, it follows that the optimal CAVI approximation is to take $\hat{q}^{(r)}(z_i) = \text{Categorical} \left(z_i; \tau_i^{(r)} \right)$, where

$$\begin{aligned}
 \tau_{ik}^{(r)} \propto \exp \left\{ \sum_{j \in \mathcal{V}} \sum_{m \in \mathcal{K}} \tau_{jm}^{(r-1)} \left[\sigma_{ij}^{(r-1)} x_{ij}(I_r) \left(\psi \left(\alpha_{km}^{(r-1)} \right) - \log \left(\beta_{km}^{(r-1)} \right) \right) + \right. \right. \\
 \sigma_{ji}^{(r-1)} x_{ji}(I_r) \left(\psi \left(\alpha_{mk}^{(r-1)} \right) - \log \left(\beta_{mk}^{(r-1)} \right) \right) - \Delta \left(\sigma_{ij}^{(r-1)} \frac{\alpha_{km}^{(r-1)}}{\beta_{km}^{(r-1)}} + \sigma_{ji}^{(r-1)} \frac{\alpha_{mk}^{(r-1)}}{\beta_{mk}^{(r-1)}} \right) \Big] \times \\
 \left(1 - \mathbb{I}_{\{k\}}(m) \mathbb{I}_{\{i\}}(j) \right) + \sigma_{ii}^{(r-1)} \left(x_{ii}(I_r) \left(\psi \left(\alpha_{kk}^{(r-1)} \right) - \log \left(\beta_{kk}^{(r-1)} \right) \right) - \Delta \frac{\alpha_{kk}^{(r-1)}}{\beta_{kk}^{(r-1)}} \right) + \\
 \left. \delta_z \left[\psi \left(\gamma_k^{(r-1)} \right) - \psi \left(\sum_{\ell} \gamma_{\ell}^{(r-1)} \right) \right] \right\},
 \end{aligned}$$

for $i \in \mathcal{V}$ and $k \in \mathcal{K}$.

B.2 Approximation of $q(\lambda_{km})$

Ignoring any terms that do not contain λ_{km} , we can derive the expectation as follows:

$$\begin{aligned}
 \mathbb{E}_{-\lambda_{km}} \{\log p(x, z, z', a, \lambda, \rho, \pi, \mu)\} &= \mathbb{E}_{-\lambda_{km}} \left\{ \log p(x|z, a, \lambda) + \delta_{\lambda} \log p(\lambda) \right\} + \text{cst.} \\
 &= \sum_{(i,j) \in \mathcal{R}} \mathbb{E}_{z_i} \{\tilde{z}_{ik}\} \mathbb{E}_{z_j} \{\tilde{z}_{jm}\} \mathbb{E}_{a_{ij}} \{a_{ij}\} \left(x_{ij}(I_r) \log \lambda_{km} - \Delta \lambda_{km} \right) + \\
 &\quad \delta_{\lambda} \left(\left(\alpha_{km}^{(r-1)} - 1 \right) \log \lambda_{km} - \beta_{km}^{(r-1)} \lambda_{km} \right) + \text{cst.} \\
 &= \left(\sum_{(i,j) \in \mathcal{R}} \mathbb{E}_{z_i} \{\tilde{z}_{ik}\} \mathbb{E}_{z_j} \{\tilde{z}_{jm}\} \mathbb{E}_{a_{ij}} \{a_{ij}\} x_{ij}(I_r) + \delta_{\lambda} \left(\alpha_{km}^{(r-1)} - 1 \right) \right) \log \lambda_{km} - \\
 &\quad \left(\Delta \sum_{(i,j) \in \mathcal{R}} \mathbb{E}_{z_i} \{\tilde{z}_{ik}\} \mathbb{E}_{z_j} \{\tilde{z}_{jm}\} \mathbb{E}_{a_{ij}} \{a_{ij}\} + \delta_{\lambda} \beta_{km}^{(r-1)} \right) \lambda_{km} + \text{cst.}
 \end{aligned}$$

Using the distributions derived for $\hat{q}^{(r-1)}(z_i)$ and assumed form for $\hat{q}^{(r-1)}(a_{ij})$, we see that the optimal CAVI approximating distribution is $\hat{q}^{(r)}(\lambda_{km}) = \text{Gamma} \left(\lambda_{km}; \alpha_{km}^{(r)}, \beta_{km}^{(r)} \right)$ with

$$\alpha_{km}^{(r)} = \delta_{\lambda} \left(\alpha_{km}^{(r-1)} - 1 \right) + \sum_{(i,j) \in \mathcal{R}} \tau_{ik}^{(r-1)} \tau_{jm}^{(r-1)} \sigma_{ij}^{(r-1)} x_{ij}(I_r) + 1,$$

$$\beta_{km}^{(r)} = \delta_\lambda \beta_{km}^{(r-1)} + \Delta \sum_{(i,j) \in \mathcal{R}} \tau_{ij}^{(r-1)} \tau_{jm}^{(r-1)} \sigma_{ij}^{(r-1)},$$

for $k, m \in \mathcal{K}$.

B.3 Approximation of $q(\rho_{k'm'})$

Ignoring any terms that do not contain $\rho_{k'm'}$, we derive the expectation as:

$$\begin{aligned} \mathbb{E}_{-\rho_{k'm'}} \{\log p(x, z, z', a, \lambda, \rho, \pi, \mu)\} &= \mathbb{E}_{-\rho_{k'm'}} \{\log p(a|z, \rho) + \delta_\rho \log p(\rho)\} + \text{cst.} \\ &= \sum_{(i,j) \in \mathcal{R}} \mathbb{E}_{z'_i} \{\tilde{z}'_{ik'}\} \mathbb{E}_{z'_j} \{\tilde{z}'_{jm'}\} \left[\mathbb{E}_{a_{ij}} \{a_{ij}\} \log \rho_{k'm'} + \mathbb{E}_{a_{ij}} \{1 - a_{ij}\} \log(1 - \rho_{k'm'}) \right] + \\ &\quad \delta_\rho \left(\eta_{k'm'}^{(r-1)} - 1 \right) \log \rho_{k'm'} + \delta_\rho \left(\zeta_{k'm'}^{(r-1)} - 1 \right) \log(1 - \rho_{k'm'}) + \text{cst.} \\ &= \left[\sum_{(i,j) \in \mathcal{R}} \mathbb{E}_{z'_i} \{\tilde{z}'_{ik'}\} \mathbb{E}_{z'_j} \{\tilde{z}'_{jm'}\} \mathbb{E}_{a_{ij}} \{a_{ij}\} + \delta_\rho \left(\eta_{k'm'}^{(r-1)} - 1 \right) \right] \log \rho_{k'm'} + \\ &\quad \left[\sum_{(i,j) \in \mathcal{R}} \mathbb{E}_{z'_i} \{\tilde{z}'_{ik'}\} \mathbb{E}_{z'_j} \{\tilde{z}'_{jm'}\} \mathbb{E}_{a_{ij}} \{1 - a_{ij}\} + \delta_\rho \left(\zeta_{k'm'}^{(r-1)} - 1 \right) \right] \log(1 - \rho_{k'm'}) + \text{cst.} \end{aligned}$$

Taking the exponential and computing expectations with respect to the derived distributions for $\hat{q}^{(r-1)}(z'_i)$ and the assumed form for $\hat{q}^{(r-1)}(a_{ij})$, it follows that the optimal CAVI approximation takes $\hat{q}^{(r)}(\rho_{k'm'}) = \text{Beta}\left(\rho_{k'm'}; \eta_{k'm'}^{(r)}, \zeta_{k'm'}^{(r)}\right)$, with

$$\begin{aligned} \eta_{k'm'}^{(r)} &= \delta_\rho \left(\eta_{k'm'}^{(r-1)} - 1 \right) + \sum_{(i,j) \in \mathcal{R}} \nu_{ik'}^{(r-1)} \nu_{jm'}^{(r-1)} \sigma_{ij} + 1, \\ \zeta_{k'm'}^{(r)} &= \delta_\rho \left(\zeta_{k'm'}^{(r-1)} - 1 \right) + \sum_{(i,j) \in \mathcal{R}} \nu_{ik'}^{(r-1)} \nu_{jm'}^{(r-1)} (1 - \sigma_{ij}^{(r-1)}) + 1, \end{aligned}$$

for $k', m' \in \mathcal{K}'$.

B.4 Approximation of $q(\pi)$

Ignoring any terms that do not contain π , we derive the expectation as:

$$\begin{aligned} \mathbb{E}_{-\pi} \{\log p(x, z, z', a, \lambda, \rho, \pi, \mu)\} &= \mathbb{E}_{-\pi} \{\delta_z \log p(z|\pi) + \delta_\pi \log p(\pi)\} \\ &= \mathbb{E}_{-\pi} \left\{ \delta_z \sum_{i \in \mathcal{V}} \sum_{k \in \mathcal{K}} \tilde{z}_{ik} \log \pi_k + \delta_\pi \sum_{k \in \mathcal{K}} \left(\gamma_k^{(r-1)} - 1 \right) \log \pi_k \right\} + \text{cst.} \\ &= \sum_{k \in \mathcal{K}} \left\{ \sum_{i \in \mathcal{V}} \mathbb{E}_{z_i} \{\tilde{z}_{ik}\} + \delta_\pi \left(\gamma_k^{(r-1)} - 1 \right) \right\} \log \pi_k + \text{cst.} \end{aligned}$$

Using the derived forms for $\hat{q}^{(r-1)}(z_i)$, we see that the optimal CAVI choice is $\hat{q}^{(r)}(\pi) = \text{Dirichlet}(\pi; \gamma^{(r)})$, where

$$\gamma_k^{(r)} = \delta_\pi \left(\gamma_k^{(r-1)} - 1 \right) + \delta_z \sum_{i \in \mathcal{V}} \tau_{ik}^{(r-1)} + 1,$$

for $k \in \mathcal{K}$.

B.5 Approximation of $q(\mu)$

Ignoring any terms that do not contain μ , we compute the necessary expectation as:

$$\begin{aligned}\mathbb{E}_{-\mu}\{\log p(x, z, z', a, \lambda, \rho, \pi, \mu)\} &= \mathbb{E}_{-\mu}\{\log p(z'|\mu) + \delta_\mu \log p(\mu)\} \\ &= \mathbb{E}_{-\mu}\left\{\sum_{i \in \mathcal{V}} \sum_{k' \in \mathcal{K}'} \tilde{z}'_{ik'} \log \mu_{k'} + \delta_\mu \sum_{k' \in \mathcal{K}'} \left(\xi_{k'}^{(r-1)} - 1\right) \log \mu_{k'}\right\} + \text{cst.} \\ &= \sum_{k' \in \mathcal{K}'} \left\{\sum_{i \in \mathcal{V}} \mathbb{E}_{z'_i}\{\tilde{z}'_{ik'}\} + \delta_\mu \left(\xi_{k'}^{(r-1)} - 1\right)\right\} \log \mu_{k'} + \text{cst.}\end{aligned}$$

Taking the exponential, and using the derived form for $\hat{q}^{(r-1)}(z'_i)$, we see that the optimal CAVI distribution is $\hat{q}^{(r)}(\mu) = \text{Dirichlet}(\mu; \xi^{(r)})$, where

$$\xi_{k'}^{(r)} = \delta_\mu \left(\mu_{k'}^{(r-1)} - 1\right) + \sum_{i \in \mathcal{V}} \nu_{ik'}^{(r-1)} + 1,$$

for $k' \in \mathcal{K}$.

B.6 Approximation of $q(z'_i)$

Ignoring terms that do not contain z'_i , we derive the expectation as:

$$\begin{aligned}\mathbb{E}_{-z'_i}\{\log p(x, z, z', a, \lambda, \rho, \pi, \mu)\} &= \mathbb{E}_{-z'_i}\{\log p(a|z', \rho) + \log p(z'|\mu)\} + \text{cst.} \\ &= \mathbb{E}_{-z'_i}\left\{\sum_{i', j' \in \mathcal{V}} \sum_{k', m' \in \mathcal{K}'} \tilde{z}'_{ik'} \tilde{z}'_{jm'} \left[a_{i'j'} \log \rho_{k'm'} + (1 - a_{i'j'}) \log(1 - \rho_{k'm'})\right] + \sum_{k' \in \mathcal{K}'} \tilde{z}'_{ik'} \log \mu_{k'}\right\} + \text{cst.} \\ &= \mathbb{E}_{-z'_i}\left\{\sum_{j \in \mathcal{V}} \sum_{k', m' \in \mathcal{K}'} \tilde{z}'_{jk'} \tilde{z}'_{im'} \left[a_{ij} \log \rho_{k'm'} + (1 - a_{ij}) \log(1 - \rho_{k'm'})\right] + \right. \\ &\quad \sum_{j' \in \mathcal{V}} \sum_{k', m' \in \mathcal{K}'} \tilde{z}'_{ik'} \tilde{z}'_{jm'} \left[a_{j'i} \log \rho_{k'm'} + (1 - a_{j'i}) \log(1 - \rho_{k'm'})\right] - \\ &\quad \left. \sum_{k' \in \mathcal{K}'} \tilde{z}'_{ik'} \left[a_{ii} \log \rho_{k'k'} + (1 - a_{ii}) \log(1 - \rho_{k'k'})\right] + \sum_{k' \in \mathcal{K}'} \tilde{z}'_{ik'} \log \mu_{k'}\right\} + \text{cst.} \\ &= \sum_{k' \in \mathcal{K}'} \tilde{z}'_{ik'} \left\{\sum_{j \in \mathcal{V}} \sum_{m' \in \mathcal{K}'} \tilde{z}'_{jm'} \left[\mathbb{E}_{a_{ij}}\{a_{ij}\} \mathbb{E}_{\rho_{k'm'}}\{\log \rho_{k'm'}\} + \mathbb{E}_{a_{ij}}\{1 - a_{ij}\} \mathbb{E}_{\rho_{k'm'}}\{\log(1 - \rho_{k'm'})\} + \right. \right. \\ &\quad \left. \mathbb{E}_{a_{ji}}\{a_{ji}\} \mathbb{E}_{\rho_{m'k'}}\{\log \rho_{m'k'}\} + \mathbb{E}_{a_{ji}}\{1 - a_{ji}\} \mathbb{E}_{\rho_{m'k'}}\{\log(1 - \rho_{m'k'})\}\right] \left(1 - \mathbb{I}_{\{k'\}}(m') \mathbb{I}_{\{i\}}(j)\right) + \\ &\quad \left. \mathbb{E}_{a_{ii}}\{a_{ii}\} \mathbb{E}_{\rho_{k'k'}}\{\log \rho_{k'k'}\} + \mathbb{E}_{a_{ii}}\{1 - a_{ii}\} \mathbb{E}_{\rho_{k'k'}}\{\log(1 - \rho_{k'k'})\} + \mathbb{E}_{\mu_{k'}}\{\log \mu_{k'}\}\right\} + \text{cst.}\end{aligned}$$

Taking the exponential, and using the distributions derived for $\hat{q}^{(r-1)}(\rho_{k'm'})$ and the assumed form of $\hat{q}^{(r-1)}(a_{ij})$, it follows that the optimal CAVI choice of $\hat{q}^{(r)}(z'_i)$ is $\hat{q}^{(r)}(z'_i) = \text{Categorical}(z'_i; \nu_i)$, where

$$\begin{aligned}\nu_{ik'}^{(r)} &\propto \exp \left\{\sum_{j \in \mathcal{V}} \sum_{m' \in \mathcal{K}'} \nu_{jm'}^{(r-1)} \left[\sigma_{ij}^{(r-1)} \left(\psi\left(\eta_{k'm'}^{(r-1)}\right) - \psi\left(\eta_{k'm'}^{(r-1)} + \zeta_{k'm'}^{(r-1)}\right)\right) + \right. \right. \\ &\quad \left. \left(1 - \sigma_{ij}^{(r-1)}\right) \left(\psi\left(\zeta_{k'm'}^{(r-1)}\right) - \psi\left(\eta_{k'm'}^{(r-1)} + \zeta_{k'm'}^{(r-1)}\right)\right) + \sigma_{ji}^{(r-1)} \left(\psi\left(\eta_{m'k'}^{(r-1)}\right) - \psi\left(\eta_{m'k'}^{(r-1)} + \zeta_{m'k'}^{(r-1)}\right)\right) + \right. \\ &\quad \left. \left(1 - \sigma_{ji}^{(r-1)}\right) \left(\psi\left(\zeta_{m'k'}^{(r-1)}\right) - \psi\left(\eta_{m'k'}^{(r-1)} + \zeta_{m'k'}^{(r-1)}\right)\right) + \sigma_{ii}^{(r-1)} \left(\psi\left(\eta_{k'k'}^{(r-1)}\right) - \psi\left(\eta_{k'k'}^{(r-1)} + \zeta_{k'k'}^{(r-1)}\right)\right) + \right. \\ &\quad \left. \left(1 - \sigma_{ii}^{(r-1)}\right) \left(\psi\left(\zeta_{k'k'}^{(r-1)}\right) - \psi\left(\eta_{k'k'}^{(r-1)} + \zeta_{k'k'}^{(r-1)}\right)\right) + \psi\left(\mu_{k'}\right) - \psi\left(\mu_{k'} + \zeta_{k'k'}^{(r-1)}\right)\right\}\end{aligned}$$

$$\begin{aligned}
 & \left(1 - \sigma_{ji}^{(r-1)}\right) \left(\psi \left(\zeta_{m'k'}^{(r-1)} \right) - \psi \left(\eta_{m'k'}^{(r-1)} + \zeta_{m'k'}^{(r-1)} \right) \right) \left(1 - \mathbb{I}_{\{k'\}}(m') \mathbb{I}_{\{i\}}(j) \right) + \\
 & \sigma_{ii}^{(r-1)} \left(\psi \left(\eta_{k'k'}^{(r-1)} \right) - \psi \left(\eta_{k'k'}^{(r-1)} + \zeta_{k'k'}^{(r-1)} \right) \right) + \left(1 - \sigma_{ii}^{(r-1)}\right) \left(\psi \left(\zeta_{k'k'}^{(r-1)} \right) - \psi \left(\eta_{k'k'}^{(r-1)} + \zeta_{k'k'}^{(r-1)} \right) \right) + \\
 & \psi \left(\xi_{k'}^{(r-1)} \right) - \psi \left(\sum_{\ell} \xi_{\ell}^{(r-1)} \right) \Big\},
 \end{aligned}$$

for $i \in \mathbb{V}$ and $k' \in \mathcal{K}'$.

Appendix C Derivation of CAVI updates for the Dirichlet process prior

Under our model specification, the term for $\log p(z_i|u)$ can be rewritten using indicators as

$$\log p(z_i|u) = \sum_{\ell=1}^{\infty} \left[\mathbb{I}\{z_i = \ell\} \log(u_{\ell}) + \mathbb{I}\{z_i > \ell\} \log(1 - u_{\ell}) \right].$$

The joint loglikelihood then becomes

$$\begin{aligned}
 \log p(x, z, u, \lambda) &= (\nu - 1) \sum_{\ell=1}^{\infty} \log(1 - u_{\ell}) + (\alpha_{km} - 1) \sum_{k,m=1}^{\infty} \left[\log(\lambda_{km}) - \beta_{km} \lambda_{km} \right] + \\
 & \sum_{i \in \mathcal{V}} \sum_{\ell=1}^{\infty} \left[\mathbb{I}\{z_i = \ell\} \log(u_{\ell}) + \mathbb{I}\{z_i > \ell\} \log(1 - u_{\ell}) \right] + \\
 & \sum_{(i,j) \in \mathcal{E}} \sum_{k,m=1}^{\infty} \tilde{z}_{ik} \tilde{z}_{jm} \left[x_{ij}(I_r) \log(\lambda_{km}) - \Delta \lambda_{km} \right] + \text{cst.}
 \end{aligned}$$

C.1 Approximation of $q(z_i)$

Recalling that $q(u_L = 1) = 1$, it follows that $\mathbb{I}\{z_i > L\} = 0$. We can thus compute the necessary expectation as:

$$\begin{aligned}
 \mathbb{E}_{-z_i} \{ \log p(x, z, u, \lambda) \} &= \mathbb{E}_{-z_i} \left\{ \delta_z \sum_{\ell=1}^L \left[\mathbb{I}\{z_i = \ell\} \log(u_{\ell}) + \mathbb{I}\{z_i > \ell\} \log(1 - u_{\ell}) \right] + \right. \\
 & \sum_{j:(i,j) \in \mathcal{E}} \sum_{k,m=1}^L \tilde{z}_{ik} \tilde{z}_{jm} \left(x_{ij}(I_r) \log(\lambda_{km}) - \Delta \lambda_{km} \right) + \\
 & \sum_{j':(j',i) \in \mathcal{E}} \sum_{k,m=1}^L \tilde{z}_{j'k} \tilde{z}_{im} \left(x_{j'i}(I_r) \log(\lambda_{km}) - \Delta \lambda_{km} \right) - \sum_{k=1}^L \tilde{z}_{ik} \left(x_{ii}(t) \log(\lambda_{kk}) - \Delta \lambda_{kk} \right) \Big\} + \text{cst.} \\
 &= \sum_{k=1}^L \tilde{z}_{ik} \left\{ \delta_z \left[\mathbb{E}_{u_k} \{ \log(u_k) \} + \sum_{\ell=1}^{k-1} \mathbb{E}_{u_{\ell}} \{ \log(1 - u_{\ell}) \} \right] + x_{ii}(t) \mathbb{E}_{\lambda_{kk}} \{ \log(\lambda_{kk}) \} - \Delta \mathbb{E}_{\lambda_{kk}} \{ \lambda_{kk} \} + \right. \\
 & \sum_{m=1}^L \left[\sum_{j:(i,j) \in \mathcal{E}} \mathbb{E}_{z_j} \{ \tilde{z}_{jm} \} \left(x_{ij}(I_r) \mathbb{E}_{\lambda_{km}} \{ \log(\lambda_{km}) \} - \Delta \mathbb{E}_{\lambda_{km}} \{ \lambda_{km} \} \right) \left(1 - \mathbb{I}_{\{k\}}(m) \mathbb{I}_{\{i\}}(j) \right) + \right. \\
 & \left. \left. \sum_{j':(j',i) \in \mathcal{E}} \mathbb{E} \{ \tilde{z}_{j'm} \} \left(x_{j'i}(I_r) \mathbb{E}_{\lambda_{mk}} \{ \log(\lambda_{mk}) \} - \Delta \mathbb{E}_{\lambda_{mk}} \{ \lambda_{mk} \} \right) \left(1 - \mathbb{I}_{\{k\}}(m) \mathbb{I}_{\{i\}}(j') \right) \right] \right\} + \text{cst.}
 \end{aligned}$$

Using the distributions derived for $\hat{q}^{(r-1)}(\lambda_{km})$ and $\hat{q}^{(r-1)}(u_\ell)$, it follows that the optimal CAVI distribution is $\hat{q}^{(r)}(z_i) = \text{Categorical}(z_i; \tau_i^{(r)})$, with

$$\begin{aligned} \tau_{ik}^{(r)} \propto \exp \left\{ \delta_z \left[\psi(\omega_k^{(r-1)}) - \psi(\omega_k^{(r-1)} + \nu_k^{(r-1)}) + \sum_{\ell=1}^{k-1} \left(\psi(\nu_\ell^{(r-1)}) - \psi(\omega_\ell^{(r-1)} + \nu_\ell^{(r-1)}) \right) \right] + \right. \\ \left. x_{ii}(I_r) \left(\psi(\alpha_{kk}^{(r-1)}) - \log(\beta_{kk}^{(r-1)}) \right) - \Delta \frac{\alpha_{kk}^{(r-1)}}{\beta_{kk}^{(r-1)}} + \right. \\ \left. \sum_{m=1}^L \left[\sum_{j:(i,j) \in \mathcal{E}} \tau_{jm}^{(r-1)} \left(x_{ij}(I_r) \left(\psi(\alpha_{km}^{(r-1)}) - \log(\beta_{km}^{(r-1)}) \right) - \Delta \frac{\alpha_{km}^{(r-1)}}{\beta_{km}^{(r-1)}} \right) \left(1 - \mathbb{I}_{\{k\}}(m) \mathbb{I}_{\{i\}}(j) \right) + \right. \right. \\ \left. \left. \sum_{j':(j',i) \in \mathcal{E}} \tau_{j'm}^{(r-1)} \left(x_{j'i}(I_r) \left(\psi(\alpha_{mk}^{(r-1)}) - \log(\beta_{mk}^{(r-1)}) \right) - \Delta \frac{\alpha_{mk}^{(r-1)}}{\beta_{mk}^{(r-1)}} \right) \left(1 - \mathbb{I}_{\{k\}}(m) \mathbb{I}_{\{i\}}(j') \right) \right] \right\}, \end{aligned}$$

for $i \in \mathcal{V}$ and $k \in \mathcal{K}$.

C.2 Approximation of $q(\lambda_{km})$

Recall that $q(u_L = 1) = 1$, and so $\pi(u_{L+1}) = \pi(u_{L+2}) = \dots$. This truncation removes the need for an infinite sum. In this way, we can compute the expectation for the CAVI approximation as:

$$\begin{aligned} \mathbb{E}_{-\lambda_{km}} \{\log p(x, z, u, \lambda)\} &= \sum_{k,m=1}^{\infty} \mathbb{E}_{-\lambda_{km}} \left[\delta_\lambda \left(\alpha_{km}^{(r-1)} - 1 \right) \log \lambda_{km} - \delta_\lambda \beta_{km}^{(r-1)} \lambda_{km} + \right. \\ &\quad \left. \sum_{(i,j) \in \mathcal{E}} \tilde{z}_{ik} \tilde{z}_{jm} \left\{ x_{ij}(I_r) \log(\lambda_{km}) - \Delta \lambda_{km} \right\} \right] + \text{cst.} \\ &= \sum_{k,m=1}^L \left[\left(\delta_\lambda \left(\alpha_{km}^{(r-1)} - 1 \right) + \sum_{(i,j) \in \mathcal{E}} \mathbb{E}_{z_i} \{\tilde{z}_{ik}\} \mathbb{E}_{z_j} \{\tilde{z}_{jm}\} x_{ij}(I_r) \right) \log(\lambda_{km}) - \right. \\ &\quad \left. \left(\delta_\lambda \beta_{km}^{(r-1)} + \Delta \sum_{(i,j) \in \mathcal{E}} \mathbb{E}_{z_i} \{\tilde{z}_{ik}\} \mathbb{E}_{z_j} \{\tilde{z}_{jm}\} \right) \lambda_{km} \right] + \text{cst.} \end{aligned}$$

Using the derived distributions for $\hat{q}^{(r-1)}(z_i)$, it follows that the optimal CAVI approximation is $q^{(r-1)}(\lambda_{km}) = \text{Gamma}(\lambda_{km}; \alpha_{km}^{(r)}, \beta_{km}^{(r)})$, where

$$\begin{aligned} \alpha_{km}^{(r)} &= \delta_\lambda \left(\alpha_{km}^{(r-1)} - 1 \right) + \sum_{(i,j) \in \mathcal{E}} \tau_{ik}^{(r-1)} \tau_{jm}^{(r-1)} x_{ij}(I_r) + 1, \\ \beta_{km}^{(r)} &= \delta_\lambda \beta_{km}^{(r-1)} + \Delta \sum_{(i,j) \in \mathcal{E}} \tau_{ik}^{(r-1)} \tau_{jm}^{(r-1)}, \end{aligned}$$

for $k, m \in \mathcal{K}$.

C.3 Approximation of $q(u_i)$

Again, using that $q^{(r-1)}(u_L = 1) = 1$, we have $\log(1 - u_L) = 0$ and $\mathbb{I}_{\{k\}}\{z_j\} = 0$, for $k > L$, the required expectation becomes:

$$\mathbb{E}_{-u_j} \{\log p(x, z, u, \lambda)\} = \mathbb{E}_{-u_j} \left\{ \mathbb{I}\{j < L\} \left[\delta_u \left(\omega_j^{(r-1)} - 1 \right) \log(u_j) + \delta_u \left(\nu_j^{(r-1)} - 1 \right) \log(1 - u_j) + \right. \right.$$

$$\begin{aligned}
& \delta_z \sum_{i \in \mathcal{V}} \left(\mathbb{I}_{\{j\}} \{z_i\} \log(u_j) + \sum_{k > j} \mathbb{I}_{\{k\}} \{z_i\} \log(1 - u_j) \right) \Big\} + \text{cst.} \\
&= \mathbb{I}\{j < L\} \left[\log(u_j) \left(\delta_z \sum_{i \in \mathcal{V}} \tau_{ij}^{(r-1)} + \delta_u \left(\omega_j^{(r-1)} - 1 \right) \right) + \right. \\
& \quad \left. \log(1 - u_j) \left(\delta_z \sum_{i \in \mathcal{V}} \sum_{k=j+1}^L \tau_{ik}^{(r-1)} + \delta_u \left(\nu_j^{(r-1)} - 1 \right) \right) \right] + \text{cst.}
\end{aligned}$$

where we have used the derived forms for $\hat{q}^{(r-1)}(z_i)$ to compute the indicator expectations. It follows that the optimal CAVI approximation is $\hat{q}^{(r)}(u_j) = \text{Beta} \left(u_j; \omega_j^{(r)}, \nu_j^{(r)} \right)$, where

$$\begin{aligned}
\omega_j' &= \delta_z \sum_{i \in \mathcal{V}} \tau_{ij}^{(r-1)} + \delta_u \left(\omega_j^{(r-1)} - 1 \right) + 1, \\
\nu_j' &= \delta_z \sum_{i \in \mathcal{V}} \sum_{k=j+1}^L \tau_{ik}^{(r-1)} + \delta_u \left(\nu_j^{(r-1)} - 1 \right) + 1,
\end{aligned}$$

for $j \in \{1, \dots, L\}$.